https://doi.org/10.5194/bg-2020-152
Preprint. Discussion started: 15 May 2020

Biogeosciences Discussions

Assimilating synthetic Biogeochemical-Argo and ocean colour observations into a global ocean model to inform observing system design

David Ford[1]

[1]Met Office, FitzRoy Road, Exeter, EX1 3PB, UK

Correspondence: David Ford (david.ford@metoffice.gov.uk)

Abstract. A set of observing system simulation experiments has been performed to explore the impact on global ocean biogeochemical reanalyses of assimilating chlorophyll from remotely sensed ocean colour, and assess the potential impact of assimilating in situ observations of chlorophyll, nitrate, oxygen, and pH from a proposed array of Biogeochemical-Argo (BGC-Argo) floats. Two different potential BGC-Argo array distributions were tested: one where biogeochemical sensors are placed on all current Argo floats, and one where biogeochemical sensors are placed on a quarter of current Argo floats. This latter approximately corresponds to the proposed BGC-Argo array of 1000 floats. Different strategies for updating model variables when assimilating ocean colour were assessed. All similarly improved the assimilated variable surface chlorophyll, but had a mixed impact on the wider ecosystem and carbon cycle, degrading some key variables of interest. Assimilating BGC-Argo data gave no added benefit over ocean colour in terms of simulating surface chlorophyll, but for most other variables, including sub-surface chlorophyll, adding BGC-Argo greatly improved results throughout the water column. This included surface partial pressure of carbon dioxide (pCO_2), which was not assimilated but is an important output of reanalyses. Both BGC-Argo array distributions gave benefits, with greater improvements seen with more observations. From the point of view of ocean reanalysis, it is recommended to proceed with development of BGC-Argo as a priority. The proposed array of 1000 floats will lead to clear improvements in reanalyses, with a larger array likely to bring further benefits. The ocean colour satellite observing system should also be maintained, as ocean colour and BGC-Argo will provide complementary benefits. There is also much potential to improve the use of existing observations, particularly in terms of multivariate balancing, through improving assimilation methodologies.

1 Introduction

Throughout the ocean, physical and chemical processes interact with a teeming ecosystem to affect all life on Earth. The upwelling of nutrient-rich waters fuels the growth of phytoplankton, which form the base of the marine food web and contribute half the planet's primary production. Oxygen is required for marine and terrestrial life, and its availability depends on ocean circulation, solubility, and biological activity. Carbon is taken up at the sea surface, at a rate contingent on physics and biology, and transported throughout the ocean. Some is stored for centuries at vast depths, mitigating climate change. Some is quickly

https://doi.org/10.5194/bg-2020-152
Preprint. Discussion started: 15 May 2020

released back to the atmosphere. All these phenomena are regulated by an array of processes which display variability on a range of scales from milliseconds to millennia, and from nanometres to ocean basins.

Understanding, monitoring, and predicting these processes is key to addressing some of the biggest challenges facing humanity. Rising carbon dioxide (CO_2) emissions are leading to climatic changes which threaten severe impacts on people and ecosystems (IPCC, 2014). Uptake of carbon by the global ocean acts to mitigate these impacts, but the ocean carbon sink is highly variable and its future magnitude uncertain (McKinley et al., 2017). At the same time, when CO_2 dissolves in seawater it reacts with it, leading to a decrease in pH referred to as ocean acidification (Doney et al., 2009). This could have major consequences for marine life, particularly organisms which form calcium carbonate shells, which become at risk of dissolution if the seawater pH is too low. Changes in climate and eutrophication also appear to be leading to expanding "dead zones" in the ocean (Diaz and Rosenberg, 2008; Altieri and Gedan, 2015), where oxygen concentrations are too low for most organisms to survive. On shorter time-scales, primary production varies considerably due to natural climate variability such as the El Niño Southern Oscillation (ENSO), and changes can have profound impacts on higher trophic levels, and hence the fisheries and aquaculture on which an estimated 12 % of the global population rely for their livelihoods (FAO, 2016). All these factors and more are captured in a drive towards "Good Environmental Status" of national waters, as regulated by policies such as the Marine Strategy Framework Directive (MSFD) of the European Union (EU).

Comprehensively monitoring all relevant processes in the global ocean, and their variability and trends, is not a trivial task. For ocean biogeochemistry, the global observing system consists of various components which, while often sparse and disparate, have allowed fundamental insights. Two decades of routine satellite ocean colour data (Groom et al., 2019) have yielded unprecedented knowledge about phytoplankton variability (Racault et al., 2017), and even helped overturn decades of scientific consensus on bloom formation (Behrenfeld and Boss, 2014). In situ stations such as the Bermuda Atlantic Time Series (BATS) have allowed long-term monitoring of multiple variables at fixed locations (Bates et al., 2014), and various networks of ships, gliders, and moorings give ongoing views of different aspects of the global ocean (Telszewski et al., 2018). These observation networks are vital, and have transformed our understanding of ocean biogeochemistry. But they remain sparse, and coverage is insufficient to address all outstanding scientific questions, or provide comprehensive monitoring on a global scale.

Observation of ocean physics has been revolutionised by the advent of Argo (Roemmich et al., 2019). A global array of around 4000 autonomous floats drift at a typical parking depth of 1000 m, and every ten days descend to 2000 m before rising to the surface, profiling temperature and salinity as they do so. The data are then transmitted to satellites in near-real-time, before the float returns to its parking depth. Argo has facilitated breakthroughs in climate science (Wijffels et al., 2016), and improvements in physical ocean reanalyses and forecasts (Davidson et al., 2019).

The Argo initiative is now being extended to biogeochemistry through the Biogeochemical-Argo (hereafter BGC-Argo) programme (Biogeochemical-Argo Planning Group, 2016; Roemmich et al., 2019). In the next decade, it is planned to establish a global array of 1000 BGC-Argo floats, which are Argo floats equipped with biogeochemical sensors. The aim is for all these floats to measure six core variables: oxygen concentration (O_2), nitrate concentration (NO_3), pH, chlorophyll-a concentration (chl-a), suspended particles, and downwelling irradiance. This promises to transform scientific understanding of ocean biogeo-

https://doi.org/10.5194/bg-2020-152
Preprint. Discussion started: 15 May 2020

chemistry. Thanks to a series of regional programmes, there are already over 300 operational floats measuring one or more biogeochemical variables. Few of these floats yet measure all the core BGC-Argo variables, and spatial coverage is highly uneven, but important scientific discoveries regarding phytoplankton, carbon, and nutrient dynamics have been made (Roemmich et al., 2019).

The value of observations can be further enhanced by combining them with numerical models using data assimilation (Kalnay, 2003). Ocean colour data are increasingly assimilated in state-of-the-art reanalysis (Rousseaux and Gregg, 2015; Ciavatta et al., 2016; Ford and Barciela, 2017) and forecasting (Teruzzi et al., 2014; Skákala et al., 2018) systems. This has consistently been shown to improve simulations of phytoplankton, but the impact on other model variables, especially subsurface, is limited (Gehlen et al., 2015). Physical data assimilation has the potential to improve biogeochemistry, but has often been found to have the opposite effect, due to spurious impacts on vertical mixing to which biogeochemical variables are particularly sensitive (Park et al., 2018; Raghukumar et al., 2015). Assimilating multivariate in situ biogeochemical data should help address these issues and greatly improve reanalyses and forecasts (Yu et al., 2018), but due to the sparsity of observational coverage, efforts have largely been limited to parameter estimation (Schartau et al., 2017), 1D models (Torres et al., 2006), individual research cruises (Anderson et al., 2000), or surface-only carbon data (Valsala and Maksyutov, 2010; While et al., 2012). Furthermore, in situ biogeochemical observations are rarely available in near-real-time, limiting their suitability for operational applications.

The increasing availability of BGC-Argo data promises to change this, with great potential for improving reanalyses and forecasts (Fennel et al., 2019). For instance, BGC-Argo observations of O_2 in the Southern Ocean have been assimilated by Verdy and Mazloff (2017), and Cossarini et al. (2019) have assimilated profiles of chl-a in the Mediterranean Sea.

This paper describes the development of a scheme to assimilate profiles of chl-a, NO_3, O_2, and pH into an updated version of the Met Office's global physical-biogeochemical ocean reanalysis system. A set of observing system simulation experiments (OSSEs) (Masutani et al., 2010) is presented to assess the potential value of different numbers of BGC-Argo floats.

This work forms part of a coordinated effort within the EU Horizon 2020 research project AtlantOS (https://www.atlantos-h2020.eu). AtlantOS had the aim of transforming various loosely-coordinated components into a "sustainable, efficient, and fit-for-purpose" Integrated Atlantic Ocean Observing System (IAOOS), consistent with the Framework for Ocean Observing (Lindstrom et al., 2012). One work package focussed on observing system design studies, using OSSEs to assess potential future improvements to existing and forthcoming components of the IAOOS. Four groups performed OSSEs assessing physics observations, the results of which have been synthesised by Gasparin et al. (2019). Two groups performed OSSEs assessing biogeochemistry, the Institute of Environmental Geosciences (IGE), and the Met Office. The IGE experiments have been published by Germineaud et al. (2019), and the Met Office experiments are presented here.

The biogeochemistry OSSEs consider two potential scenarios: 1) a global BGC-Argo array equivalent to having biogeochemical sensors on one in four existing Argo floats, which is comparable to the planned target of 1000 floats, and 2) a global BGC-Argo array equivalent to having biogeochemical sensors on all existing Argo floats. The aims were to assess the impact on reanalysis and forecasting systems that might be seen by assimilating multivariate BGC-Argo data, the influence of array size, and the value BGC-Argo would add to the existing ocean colour satellite constellation. Assimilation of physics variables

https://doi.org/10.5194/bg-2020-152
Preprint. Discussion started: 15 May 2020

was not included, due to the issues mentioned above, and reflecting the way state-of-the-art biogeochemical reanalyses are run (Fennel et al., 2019).

This paper describes the updated model and newly-developed assimilation scheme, and setup of the OSSEs. Results are presented exploring ways to use ocean colour data assimilation to make multivariate updates, and combine it with in situ chl-a profiles. Results are then presented showing the impact of assimilating the two potential BGC-Argo arrays. Finally, recommendations are made for the future development of observing and assimilation systems.

2 Model and assimilation

The reanalysis system is an upgraded version of that used in previous biogeochemical data assimilation studies at the Met Office (Ford et al., 2012; While et al., 2012; Ford and Barciela, 2017; Ford, 2019).

2.1 Model

The physical ocean model used is the GO6 configuration (Storkey et al., 2018) of the Nucleus for European Modelling of the Ocean (NEMO) hydrodynamic model (Madec, 2008), using the extended ORCA025 tripolar grid, which has a horizontal resolution of 1/4° and 75 vertical levels. This is coupled online to the GSI8.1 configuration (Ridley et al., 2018) of the Los Alamos Sea Ice Model (CICE) (Hunke et al., 2015). Together, these form the ocean and sea ice components of the GC3.1 configuration (Williams et al., 2017) of the Hadley Centre Global Environment Model version 3 (HadGEM3), which is used for physical climate simulations submitted to the Coupled Model Intercomparison Project Phase 6 (CMIP6) (Eyring et al., 2016). When combined with the physics version of the data assimilation scheme described below, the ocean and sea ice models are also used in version 14 of the Forecasting Ocean Assimilation Model (FOAM), earlier versions of which are described by Blockley et al. (2014) and Storkey et al. (2010). FOAM is run operationally at the Met Office to produce short-range forecasts of the physical ocean and sea ice state. It is also used to initialise the ocean and sea ice components of the Met Office Global Seasonal forecasting system version 5 (GloSea5) (MacLachlan et al., 2015; Scaife et al., 2014), and short-range coupled ocean–atmosphere forecasting system (Guiavarc'h et al., 2019).

The biogeochemical ocean model used in this study is version 2 of the Model of Ecosystem Dynamics, nutrient Utilisation, Sequestration and Acidification (MEDUSA) (Yool et al., 2013). MEDUSA is of intermediate complexity, representing two phytoplankton and two zooplankton types, with a variable carbon to chlorophyll ratio and a coupled carbon cycle. This differs from previous versions of the Met Office physical-biogeochemical ocean reanalysis system (Ford and Barciela, 2017), which used the Hadley Centre Ocean Carbon Cycle Model (HadOCC) (Palmer and Totterdell, 2001). This is because, following an intercomparison (Kwiatkowski et al., 2014) of biogeochemical models developed in the UK, MEDUSA was chosen to be the ocean biogeochemical component of version 1 of the UK Earth System Model (UKESM1) (Sellar et al., 2019). UKESM1 consists of a lower-resolution version of GC3.1, coupled with models of ocean biogeochemistry, atmospheric chemistry and aerosols, and ice-sheets, and is used for Earth system climate simulations submitted to CMIP6. Using the same model versions

https://doi.org/10.5194/bg-2020-152
Preprint. Discussion started: 15 May 2020

for forecasting, reanalysis, and climate simulations provides a seamless framework for simulating the Earth system (Martin et al., 2010).

2.2 Assimilation

2.2.1 Overview

The data assimilation scheme used here is version 5 of NEMOVAR (Weaver et al., 2003, 2005; Mogensen et al., 2009, 2012), following the implementation for assimilating physical variables into the global FOAM system (Waters et al., 2015), and for assimilating ocean colour data into HadOCC (Ford, 2019) and the European Regional Seas Ecosystem Model (ERSEM) (Skákala et al., 2018). As detailed in Waters et al. (2015), this implementation of NEMOVAR uses a first guess at appropriate time (FGAT) 3D-Var methodology. A conjugate gradient algorithm is used to iteratively minimise the cost function

$$J(\delta\mathbf{x}) = \frac{1}{2}\delta\mathbf{x}^{\mathrm{T}}\mathbf{B}^{-1}\delta\mathbf{x} + \frac{1}{2}(\mathbf{d} - \mathbf{H}\delta\mathbf{x})^{\mathrm{T}}\mathbf{R}^{-1}(\mathbf{d} - \mathbf{H}\delta\mathbf{x}) \quad (1)$$

where the increment $\delta\mathbf{x} = \mathbf{x} - \mathbf{x}_{\mathrm{b}}$ is the difference between the state vector $\mathbf{x}$ and its background estimate $\mathbf{x}_{\mathrm{b}}$, the innovation vector $\mathbf{d} = \mathbf{y} - H(\mathbf{x}_i)$ is the difference between the observation vector $\mathbf{y}$ and $\mathbf{x}_i = \mathbf{M}_{\mathrm{t}_0\rightarrow\mathrm{t}_i}(\mathbf{x}_{\mathrm{b}})$, where $\mathbf{M}_{\mathrm{t}_0\rightarrow\mathrm{t}_i}$ is the nonlinear propagation model that propagates the background state to the state at time i, operated on by the observation operator H, $\mathbf{H}$ is the linearised observation operator, $\mathbf{B}$ is the background error covariance matrix, and $\mathbf{R}$ is the observation error covariance matrix. A diffusion operator is used to efficiently model spatial correlations (Mirouze et al., 2016). The observation operator forms part of the NEMO code, and computes model values in observation space by interpolating model fields to observation locations at the closest model time step to the time each observation was made. The observation operator was extended in this study to work for 3D biogeochemical variables as well as physical variables.

When applied to physics data, NEMOVAR decomposes the full multivariate background error covariance matrix into an unbalanced and a balanced component for each variable. The balanced component is derived using a set of linearised balance operators, based on physical relationships (Weaver et al., 2005; Mogensen et al., 2012). In this study, NEMOVAR has been applied to biogeochemical variables with no multivariate relationships applied, and the cost function is minimised separately for each assimilated variable. Development of biogeochemical balance relationships within NEMOVAR could be expected to bring improved results, but this would be a major development to NEMOVAR. The aim of this study was to develop an initial implementation that could be used with BGC-Argo data, and that can be further developed as systems mature.

All increments are applied to the model over one day using incremental analysis updates (IAU) (Bloom et al., 1996), which applies an equal proportion of the increments at each model time step, in order to reduce initialisation shocks.

NEMOVAR is used in this study to assimilate simulated ocean colour and BGC-Argo data, as described in the following sections. NEMOVAR can be used for combined physical–biogeochemical assimilation (Ford, 2019), but physics data is not assimilated in this study.

https://doi.org/10.5194/bg-2020-152
Preprint. Discussion started: 15 May 2020

155 **2.2.2 Ocean colour**

NEMOVAR is used here to assimilate total surface $\log_{10}$(chl-a) from ocean colour. Since MEDUSA simulates chl-a for two phytoplankton types, diatoms and non-diatoms, these are summed by the observation operator to give total chl-a, to match the input observations. Log-transformation is performed in order to give a more Gaussian error distribution (Campbell, 1995). The background and observation error covariances used are the same as in Ford (2019). In the horizontal, a correlation length-scale
160 based on the first baroclinic Rossby radius is used, consistent with Waters et al. (2015).

For surface data, such as ocean colour, NEMOVAR can be applied in one of two ways:

1. The first, which is computationally most efficient, is to calculate a set of 2D surface increments. These can then be applied equally through the mixed layer, as in Ford (2019) and Skákala et al. (2018).

2. The second is to calculate a set of 3D increments, with information from the surface observations propagated downwards
165 using vertical correlation length-scales, as described by Waters et al. (2015) for physical variables. The sub-surface background error standard deviations are parameterised based on the vertical gradient of density with depth to allow a flow-dependent vertical structure to the errors. The vertical correlation length-scale is dependent on the model's mixed layer depth: at the surface the vertical length-scale is set to the depth of the mixed layer, at the base of the mixed layer the vertical length-scale is set to a minimum value, and below the mixed layer the vertical length-scale increases with
170 the model's vertical grid resolution. This means that information from surface observations is spread to the base of the mixed layer, as determined from a one-day model forecast.

The increments applied to the model from the two methods should be similar, though not identical. The main advantage of the latter method is that it allows satellite and in situ profile observations of a given variable to be consistently combined by NEMOVAR, to produce a single set of 3D increments for that variable.

175 In each case, NEMOVAR produces a set of $\log_{10}$(chl-a) increments on the model grid (either 2D or 3D), which must be applied to the model. Various methods can be used to do this, three of which are tested here:

1. The simplest method is to convert $\log_{10}$(chl-a) increments to chl-a increments using the background total chl-a, and split this between diatoms and non-diatoms so as to conserve the ratio between the two in the background model field. This updates the model chl-a, but does not directly alter the phytoplankton biomass, effectively just changing the phytoplank-
180 ton carbon-to-chlorophyll ratio.

2. A more common approach (Teruzzi et al., 2014; Skákala et al., 2018) is to use method 1 but also update the phytoplankton biomass, by conserving the stoichiometric ratios in the background field.

3. A third method is to use the nitrogen balancing scheme of Hemmings et al. (2008), as has been routinely used with HadOCC (Ford et al., 2012). This uses a principle of conservation of mass to calculate increments to the six HadOCC
185 state variables (phytoplankton, zooplankton, dissolved inorganic nitrogen (DIN), detritus, dissolved inorganic carbon (DIC), alkalinity) at all depths. The scheme was designed and parameterised for use with HadOCC, so is not immediately

https://doi.org/10.5194/bg-2020-152
Preprint. Discussion started: 15 May 2020

compatible with the more complex and differently parameterised MEDUSA. In this study it has been extended for use with MEDUSA by summing each of the phytoplankton and zooplankton functional types to obtain total phytoplankton and zooplankton, and using these as inputs to the nitrogen balancing scheme, while maintaining the parameter values of Hemmings et al. (2008). The scheme then calculates 3D increments to phytoplankton, zooplankton, DIN, detritus, DIC, and alkalinity, which are applied to the model, with phytoplankton split into diatoms and non-diatoms, and zooplankton into meso-zooplankton and micro-zooplankton, so that the background ratios are conserved. An increment is applied to silicate that is equal and opposite to the increment applied to diatom silicon biomass, to conserve silicon. Detrital carbon is updated to preserve the ratio between detrital nitrogen and carbon in the background field. In its original form, the scheme accepts 2D surface chl-a increments, and calculates one set of increments within the mixed layer using mixed layer-averaged values of background phytoplankton biomass, growth and loss rates, then further increments beneath the mixed layer by scaling the mixed layer increments to the local background phytoplankton biomass. In this study the scheme has been further extended to accept 3D chl-a increments, and calculate a corresponding set of multivariate increments for every depth level using the background values at that depth. This allows the scheme to be used with either 2D or 3D chl-a increments from NEMOVAR.

It is not clear which of the above approaches would yield the best results with MEDUSA, so all three multivariate balancing methods have been tested, each with either 2D or 3D chl-a increments from NEMOVAR, giving six combinations as described in Section 3.

2.2.3 BGC-Argo

For in situ profiles of biogeochemistry, as might be obtained from BGC-Argo, sets of 3D increments are calculated for each assimilated variable, following the physics implementation of Waters et al. (2015). The method is the same as for calculating 3D ocean colour increments, as described above.

In this study chl-a, NO_3, O_2, and pH have been assimilated, but the methodology is simple to extend to other model variables. As for ocean colour assimilation, chl-a is the sum of diatom and non-diatom chl-a, and a log-transformation is performed prior to assimilation. As described above, assimilation of chl-a from ocean colour and in situ profiles can be combined. NO_3 and O_2 are state variables in MEDUSA, taking NO_3 to be equivalent to the MEDUSA DIN variable, while pH is a diagnostic variable calculated using version 2.0 of the mocsy carbonate package (Orr and Epitalon, 2015), which implements the SolveSAPHE algorithm (Munhoven, 2013) for solving the alkalinity-pH equation.

The chl-a increments can be applied using different multivariate balancing methods, as described for ocean colour above. The NO_3 increments are directly applied to the MEDUSA DIN variable, and the O_2 increments to the O_2 variable. As pH is a diagnostic variable, the pH increments cannot be applied directly. A similar approach is therefore taken to the assimilation of partial pressure of CO_2 (pCO_2) into HadOCC (While et al., 2012), which has also been performed with MEDUSA. pCO_2 is a function of temperature, salinity, DIC, and alkalinity, and at constant temperature and salinity constant lines of pCO_2 are found in DIC/alkalinity space (see Fig. 1 of While et al. (2012)). The scheme of While et al. (2012) assumes that temperature

https://doi.org/10.5194/bg-2020-152
Preprint. Discussion started: 15 May 2020

and salinity are error-free (and can be directly updated by physical data assimilation if not), and therefore updates DIC and alkalinity. As there is no unique combination of DIC and alkalinity that gives a specific pCO_2 value, the smallest combined change to DIC and alkalinity is made in order to reach the target pCO2 value. The same approach is taken here with pH, which is a function of temperature, salinity, nutrients, latitude, depth, DIC, and alkalinity. In DIC/alkalinity space, locally constant lines of pH are found when considering the range of present oceanic conditions (see Fig. 1a of Munhoven (2013)). The scheme developed here therefore updates DIC and alkalinity, assuming the other contributors to pH to be error-free, by making the smallest combined change which would give the target pH.

In the case where chl-a is assimilated using the nitrogen balancing scheme of Hemmings et al. (2008), and profiles of NO_3 and pH are also assimilated, this gives two different sets of increments to NO_3, DIC, and alkalinity. This combination is not used in this study, but in the current implementation precedence would be given to the increments derived from profiles of NO_3 and pH, as these are more directly related to the available observations, and just these increments applied in this situation. Ideally though, further balancing between the different variables would be applied, which can be considered as a future development.

3 Observing system simulation experiments (OSSEs)

3.1 Overview

As detailed by Masutani et al. (2010), OSSEs provide a way to test the impact on forecasts and reanalyses of assimilating observations which do not yet exist, by using synthetic observations. An OSSE typically comprises the following elements:

- A "nature run", which is a realistic non-assimilative model simulation of the real world, which provides a "truth" against which to validate the assimilative model.
- Synthetic observations representing both current and future observing networks, which are sampled from the nature run with appropriate errors prescribed.
- Optionally, a non-assimilative control run, which provides an alternative model simulation of the nature run period.
- An assimilative control run, which assimilates synthetic observations representing current observing networks into the alternative model simulation.
- One or more additional versions of the assimilative run which also assimilate synthetic observations representing the future observing networks under consideration.
- Assessment of the impact on reanalysis or forecast skill of assimilating these observations, by validating against the nature run.

One of the keys to obtaining informative results from an OSSE is to ensure that all sources of error are appropriately accounted for (Halliwell et al., 2014, 2017; Hoffman and Atlas, 2016). If the control run is more similar to the nature run

https://doi.org/10.5194/bg-2020-152
Preprint. Discussion started: 15 May 2020

than the real forecasting system is to the real world, then it can become easier for the assimilative system to recover the truth, and the impact of the observing networks may be incorrectly estimated. As such, three general OSSE approaches have been developed, which differ in how the control run varies from the nature run.

- In "identical twin experiments", the nature and control runs differ only in their initial conditions. This set-up was frequently used in early OSSEs, but as most sources of model error are neglected, the results were found to be overly optimistic, and the approach is no longer widely recommended (Arnold and Dey, 1986).
- In "fraternal twin experiments", the same model is still used for both the nature and control run, but more aspects are modified. These could include the initial conditions, lateral and surface boundary conditions, parameterisations, and resolution. This takes much better account of model errors, and the approach is recommended over identical twin experiments (Arnold and Dey, 1986; Masutani et al., 2010; Yu et al., 2019).
- In "full OSSEs", significantly different models are used for the nature and control runs, in order to make the two more independent. The nature run is often of much higher resolution than the assimilative model (Fujii et al., 2019). It is recommended to use this approach if possible (Masutani et al., 2010), but it relies on having two appropriately different models available, which is not always the case.

Due to the lack of availability of an appropriate alternative model for the nature run, it was decided within AtlantOS to take a fraternal twin approach for the biogeochemical OSSEs. This is sufficient to account for most sources of error, as long as any limitations of the approach are considered when drawing and acting upon conclusions.

3.2 Model formulation

The nature run in this study was run from 1 January 2008 to 31 December 2009, using the default parameterisations for the model versions used. This is intended to be the best available non-assimilative model representation of the real world, and validation of the general performance of different aspects of the system can be found in the references given in Section 2. Atmospheric boundary conditions were taken from the ERA-Interim reanalysis (Dee et al., 2011). Initial conditions for NEMO were taken from the end of a 30-year hindcast of GO6 (Storkey et al., 2018). Initial conditions for CICE were taken from a pre-operational trial of the FOAM v14 system. Initial conditions for MEDUSA were based on year 5000 of the initial ocean-only phase of the spin-up of UKESM1 for use in CMIP6 projections (Yool et al., 2020). As the UKESM1 spin-up was run at 1° resolution with pre-industrial atmospheric CO_2 concentrations, the UKESM1 fields were interpolated to 1/4° resolution, and the DIC and alkalinity fields replaced by the contemporary model estimates used to initialise the 1/4° resolution experiments in Ford (2019). To allow the model to settle, the first year of the nature run is treated as spin-up. The period was chosen to match OSSEs of the in situ physics observing system performed at the Met Office (Mao et al., in prep.), and more widely as part of AtlantOS (Gasparin et al., 2019).

The non-assimilative control run was performed for the same period, including spin-up, but differed from the nature run in the following ways:

https://doi.org/10.5194/bg-2020-152
Preprint. Discussion started: 15 May 2020

- Atmospheric boundary conditions were taken from the JRA-55 reanalysis (Kobayashi et al., 2015).
- NEMO initial conditions were taken from an earlier date (1 January 1999) of the hindcast of Storkey et al. (2018).
- MEDUSA initial conditions were taken from an earlier year (1218) of the UKESM1 ocean-only spin-up, with DIC and alkalinity taken from the end of the non-assimilative 1/4° resolution experiment of Ford (2019).
- The NEMO parameter rn_efr, which affects near-inertial wave breaking and therefore vertical mixing (Calvert and Siddorn, 2013), was increased from 0.05 to 0.1.
- The scheme used for advection of biogeochemical variables was changed from Total Variance Dissipation (TVD) (Zalesak, 1979) to the Monotone Upstream Scheme for Conservative Laws (MUSCL) (Van Leer, 1977; Lévy et al., 2001).
- An alternative set of MEDUSA parameters was used, specifically Parameter Set 3 from Table 2 of Hemmings et al. (2015), which was found to give differences of an appropriate magnitude.

Together, these modifications generate approximations to the errors that exist in atmospheric fluxes and simulations of ocean physics and biogeochemistry. It is important to modify all of these, as errors in atmosphere and ocean physics have significant impacts on biogeochemical reanalyses and forecasts, and these errors must be accounted for if realistic conclusions are to be drawn from the OSSEs.

3.3 Synthetic observations

Synthetic ocean colour and BGC-Argo observations were generated from the nature run for each day of 2009. Total chl-a from ocean colour represents the current observing network typically assimilated in biogeochemical reanalyses (Fennel et al., 2019). Observations were simulated at the same locations as were actually observed in 2009 in version 3.1 of the ESA CCI level three daily merged sinusoidal grid product (Sathyendranath et al., 2019), as used in recent Met Office reanalyses (Ford and Barciela, 2017). Whilst the products date from 2009 rather than present day, the observational coverage is similar, with three sensors contributing in 2009 (MERIS, MODIS, and SeaWiFS), and three contributing to recent ocean colour products (MODIS, OLCI, and VIIRS). BGC-Argo float trajectories were based on Argo float trajectories used for physics OSSEs within AtlantOS (Gasparin et al., 2019). These were generated using recent real Argo float trajectories, with modifications to ensure more even geographic coverage - for details see Gasparin et al. (2019). In this study, for testing the scenario equivalent to having biogeochemical sensors on all current standard Argo floats, the same "backbone" float trajectories were used as in the studies synthesised by Gasparin et al. (2019). For the scenario equivalent to having biogeochemical sensors on one in four Argo floats, these were subsampled using the last two digits of the float IDs. The geographic coverage in each case is shown in Fig. 1.

In data assimilation, two components of observation error are typically considered: measurement error and representation error (Janjić et al., 2018). Measurement error has been accounted for in this study by adding unbiased Gaussian noise to the nature run values at observation locations, using standard deviations from the literature. A standard deviation of 30 %

https://doi.org/10.5194/bg-2020-152
Preprint. Discussion started: 15 May 2020

Biogeosciences Discussions Open Access EGU

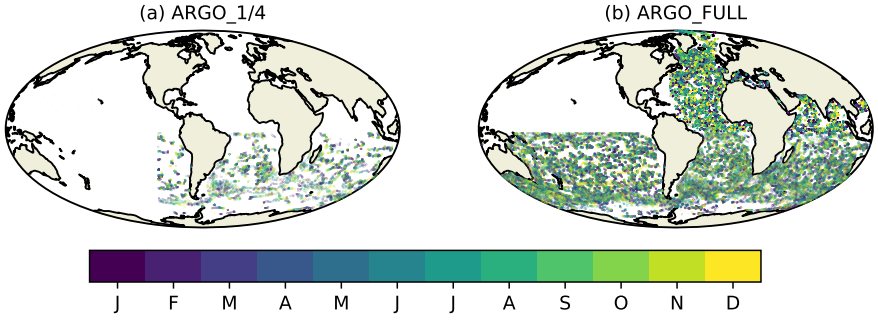

Figure 1. Simulated BGC-Argo float trajectories for 2009 equivalent to having biogeochemical sensors on (a) one in four Argo floats and (b) all Argo floats. Colours represent the month in which each observation is valid.

was agreed on within AtlantOS for chl-a from ocean colour, and the same value was also used for BGC-Argo chl-a profiles, consistent with Boss et al. (2008). For the remaining variables the values from Johnson et al. (2017) were used: 1 % for O_2, 0.005 for pH, and 0.5 mmol m^{-3} for NO_3. To avoid generating spuriously noisy profiles, a single value of Gaussian noise was calculated per profile, rather than at every depth level. Where the standard deviations used were a percentage, this was calculated using the mean of the profile.

Representation error arises from observations and models representing differing spatial and temporal scales and processes. Since the nature and control runs were at the same resolution, this was accounted for in the same way as for the physics OSSEs in AtlantOS (Gasparin et al., 2019). For each profile, the equivalent nature run values were calculated either three days before or three days after, chosen at random. The difference between these and the "truth" value were taken to be the representation error, and added on to the observation values. The advantage of this approach is that representation error is higher in more variable regions, as would be expected in real-world data assimilation applications.

3.4 Error covariances

For assimilating ocean colour data, the monthly-varying background and observation error standard deviations from Ford (2019) were used. To provide consistency between assimilating 2D and 3D $\log_{10}$(chl-a), these were also used for assimilating $\log_{10}$(chl-a) from BGC-Argo.

For other variables, pre-existing error standard deviations were not available, so were calculated for this study. Observation error standard deviations were set to a climatological constant equal to the average global observation error specified. This was 0.638 mmol m^{-3} for NO_3, 2.767 mmol m^{-3} for O_2, and 0.006 for pH. Background error standard deviations were calculated using the Canadian Quick (CQ) method (Polavarapu et al., 2005; Jackson et al., 2008), which uses the variance of the difference between successive days of a free-running model simulation as a proxy for background error variance. Annual background error standard deviations were calculated from the output of the non-assimilative control run. The CQ method is known to underestimate the magnitude of the error standard deviations (Bannister, 2008), and the results in this study were considerably lower

https://doi.org/10.5194/bg-2020-152
Preprint. Discussion started: 15 May 2020

Table 1. Experiments performed.

Identifier	Assimilation	Notes
NATURE	None	Nature run
FREE	None	Non-assimilative control run
OC_2D_CHL	Ocean colour	2D chl-a increments, only chl-a updated
OC_3D_CHL	Ocean colour	3D chl-a increments, only chl-a updated
OC_2D_PHY	Ocean colour	2D chl-a increments, biomass updated
OC_3D_PHY	Ocean colour	3D chl-a increments, biomass updated
OC_2D_NIT	Ocean colour	2D chl-a increments, nitrogen balancing
OC_3D_NIT	Ocean colour	3D chl-a increments, nitrogen balancing
ARGO_1/4_OC	1/4 Argo + ocean colour	3D chl-a increments, biomass updated
ARGO_FULL_OC	Full Argo + ocean colour	3D chl-a increments, biomass updated
ARGO_1/4	1/4 Argo	3D chl-a increments, biomass updated
ARGO_FULL	Full Argo	3D chl-a increments, biomass updated

than the observation error standard deviations used. In order to give sufficient weight to the observations for the assimilation to be effective, the background error standard deviations were inflated so that their average value matched the observation error standard deviation used. Once the system is fully functioning with real BGC-Argo data available, these estimates can be appropriately refined.

3.5 Experiments

Using these inputs, two sets of assimilation experiments were performed, in addition to the nature and non-assimilative control runs, as detailed in Table 1. The nature and non-assimilative control runs were run from 1 January 2008 to 31 December 2009, with the first year treated as spin-up. Each assimilation experiment was run from 1 January 2009 to 31 December 2009, using initial conditions from the end of the non-assimilative control run spin-up, and assimilating the synthetic observations into the version of the model used for the control run.

The first set of experiments just assimilated ocean colour, to find the most appropriate combination of vertical propagation (2D increments applied through the mixed layer or 3D increments) and multivariate balancing (chl-a only, updates to phytoplankton biomass, Hemmings et al. (2008) nitrogen balancing) for use with MEDUSA. This gave six combinations.

The second set of experiments introduced BGC-Argo, with two runs assimilating the 1/4 subsampled BGC-Argo array and the full BGC-Argo array, in combination with the chosen ocean colour scheme from the first set of experiments. A final two runs assimilated the 1/4 subsampled and full BGC-Argo arrays without ocean colour.

All the experiments, with unique identifiers for each, are detailed in Table 1.

https://doi.org/10.5194/bg-2020-152
Preprint. Discussion started: 15 May 2020

4 Results

The results are presented in three sub-sections below. The first assesses how the differences between NATURE and FREE compare to errors in real-world reanalyses. The second assesses the runs just assimilating ocean colour, while the third assesses the runs assimilating BGC-Argo. The main metric used for assessment is the percentage reduction in median absolute error (MAE), defined as:

$$\mathrm{MAE_{red}} = \frac{\mathrm{MAE_{control}} - \mathrm{MAE_{OSSE}}}{\mathrm{MAE_{control}}} \times 100 \quad (2)$$

where $\mathrm{MAE_{OSSE}}$ is the MAE of each OSSE compared with NATURE, and $\mathrm{MAE_{control}}$ is the MAE of a control run compared with NATURE. When considering the impact of data assimilation versus a free run, FREE is used as the control run, and when assessing the added value of BGC-Argo, OC_3D_PHY is used as the control run. A positive value of $\mathrm{MAE_{red}}$ represents a reduction in error in the OSSE compared to the control, and a negative value represents an increase in error. This is a modification of the approach taken by Gasparin et al. (2019), who used the percentage reduction in mean square error. MAE is used instead because the biogeochemical variables being considered are highly non-Gaussian, so it is more appropriate to use a metric such as MAE which is based on robust statistics.

4.1 Errors in free-running model

As stated in Section 3, OSSEs yield the most reliable conclusions when all sources of real-world error have been appropriately accounted for. This means that the errors between FREE and NATURE should, ideally, be broadly similar to the errors between FREE and the real world. As the real-world ocean is not known exactly, observation-based products must be used to perform this assessment, even though these can have large uncertainties and do not exactly represent the real world.

Figure 2 shows the absolute difference between FREE and an observation-based product, and between FREE and NATURE, for surface chl-a, NO_3, and pCO_2, for the final month of the simulations, December 2009. The observation-based products used are the monthly v3.1 ocean colour CCI product for chl-a (Sathyendranath et al., 2019), the 2018 World Ocean Atlas (WOA18) monthly climatology for NO_3 (Garcia et al., 2018), and the monthly pCO_2 statistical analysis product of Landschützer et al. (2015a, b). The observation-based products were bilinearly interpolated to the model grid.

For chl-a (Fig. 2a-b), the two sets of absolute difference are broadly similar in the Pacific and Southern Oceans, but in the Tropical Atlantic and Indian Oceans the absolute difference between FREE and NATURE is smaller than between FREE and the CCI data. In NATURE the chl-a in these regions was spuriously low compared with observations, linked to low nutrient concentrations. The modifications introduced in FREE served to increase nutrient concentrations in these regions, but also to suppress phytoplankton growth, resulting in little overall change in chl-a. Elsewhere though, the levels of absolute error are broadly similar, meaning the OSSEs have realistic levels of model error. While it is not ideal that the errors differ in the Tropical Atlantic and Indian Oceans, achieving globally appropriate levels of error with a complex biogeochemical model with globally uniform parameterisations could not be managed within the resources of the project. Furthermore, the similarity of NATURE

https://doi.org/10.5194/bg-2020-152
Preprint. Discussion started: 15 May 2020

Biogeosciences
Discussions
Open Access
EGU

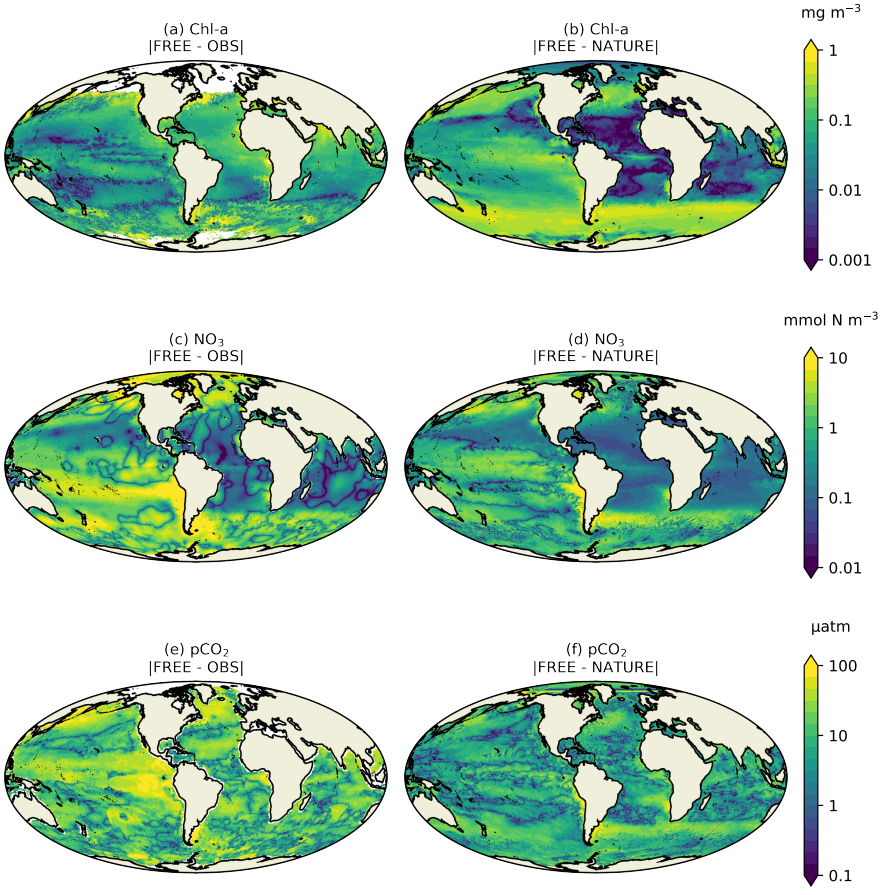

Figure 2. Absolute difference for December 2009 for surface (a-b) chl-a, (c-d) NO_3, and (e-f) pCO_2 between FREE and real-world observation-based products (left column) and between FREE and NATURE (right column).

and FREE in these regions is due to the introduction of compensating errors in FREE, rather than a lack of model error. This itself is a common feature of reanalyses, which can result in data assimilation increasing overall error by correctly reducing one of a set of compensating errors, as demonstrated by Ford and Barciela (2017).

385 For NO_3 and pCO_2 the global distributions are more similar, although the absolute difference between FREE and NATURE is slightly smaller than between FREE and the observation products, especially for pCO_2, which should be borne in mind when drawing conclusions. It should be remembered though that the observation-based products used here have large uncertainties themselves, while the comparison between FREE and NATURE does not include observation error.

https://doi.org/10.5194/bg-2020-152
Preprint. Discussion started: 15 May 2020

4.2 Ocean colour data assimilation

For each of the six runs just assimilating ocean colour using different techniques, profiles of global MAE_{red} over FREE for the last month of simulation, December 2009, are plotted in Fig. 3 for nine model variables. Profiles are plotted for the upper 250 m, approximately corresponding to the maximum depth the euphotic zone is likely to take.

For chl-a, all six runs perform very similarly at the surface, with MAE_{red} values between 67–76 %. Beneath the surface OC_2D_PHY and OC_3D_PHY perform best, reducing the MAE at all depths. OC_2D_CHL and OC_3D_CHL perform least well with some degradations to MAE below about 60 m, though it should be noted that chl-a values are extremely low at depths with insufficient light for growth, so the percentage differences between runs become less meaningful at these depths.

For phytoplankton biomass, least impact is seen in OC_2D_CHL and OC_3D_CHL, due to the biomass not being directly updated by the assimilation, with MAE_{red} values of around 7 % at the surface. The other four runs behave similarly as for chl-a, though with a smaller impact at the surface (MAE_{red} of 32–44 %) and less variation in MAE_{red} with depth. OC_2D_PHY and OC_3D_PHY give slightly better results than OC_2D_NIT and OC_3D_NIT.

For the other seven variables plotted, which are either not directly updated by the assimilation or are only updated by the Hemmings et al. (2008) balancing scheme, results are mixed. OC_2D_CHL and OC_3D_CHL have near-zero MAE_{red} values for all variables, demonstrating that just updating chl-a has very little impact on the wider model state. There are only small differences between OC_2D_PHY and OC_3D_PHY, and between OC_2D_NIT and OC_3D_NIT, suggesting that the use of NEMOVAR to create 3D increments, as required for combining assimilation of chl-a from ocean colour and BGC-Argo, is fit for purpose. Similarly, the extension of the Hemmings et al. (2008) balancing scheme to accept 3D chl-a increments as an input appears successful. The remainder of this sub-section will therefore focus on comparing OC_3D_PHY and OC_3D_NIT.

OC_3D_PHY results in a large degradation of surface zooplankton biomass and NO_3, with MAE_{red} values of -358 % and -92 % respectively. This is reduced in OC_3D_NIT to -106 % and -15 % respectively. In both runs, for zooplankton biomass MAE_{red} increases towards zero with depth. For NO_3, more complex variation in MAE_{red} is seen with depth, likely reflecting regional variations in the impact of the two assimilation strategies around the nutricline in particular. Both runs improve detrital nitrogen, with MAE_{red} values at the surface of 35 % for OC_3D_PHY and 23 % for OC_3D_NIT. MAE_{red} decreases more quickly with depth in OC_3D_PHY, but remains positive in both cases. O_2 is degraded in both runs, with a larger surface degradation in OC_3D_NIT. With the carbon cycle, DIC, alkalinity, and pH are all degraded in OC_3D_PHY. In OC_3D_NIT, DIC is further degraded near the surface, but alkalinity is now improved, with positive MAE_{red} through the water column. The result on pH, a diagnostic which is a function of DIC and alkalinity, is that OC_3D_PHY and OC_3D_NIT have a near-identical degradation in MAE_{red} of around -157 % at the surface, but OC_3D_NIT gives better results with depth.

From these results, there is not a clear indication of which multivariate balancing method gives the best overall results. It could be argued that just updating chl-a is the safest strategy, as this improves the assimilated variable (chl-a), slightly improves phytoplankton biomass, and does not degrade any other variable. It is commonly agreed though that it is highly desirable to try and use ocean colour data to improve the wider model state (Gehlen et al., 2015; Fennel et al., 2019), and this clearly cannot be achieved by solely updating chl-a. Present and future reanalyses do and will make multivariate updates,

https://doi.org/10.5194/bg-2020-152
Preprint. Discussion started: 15 May 2020

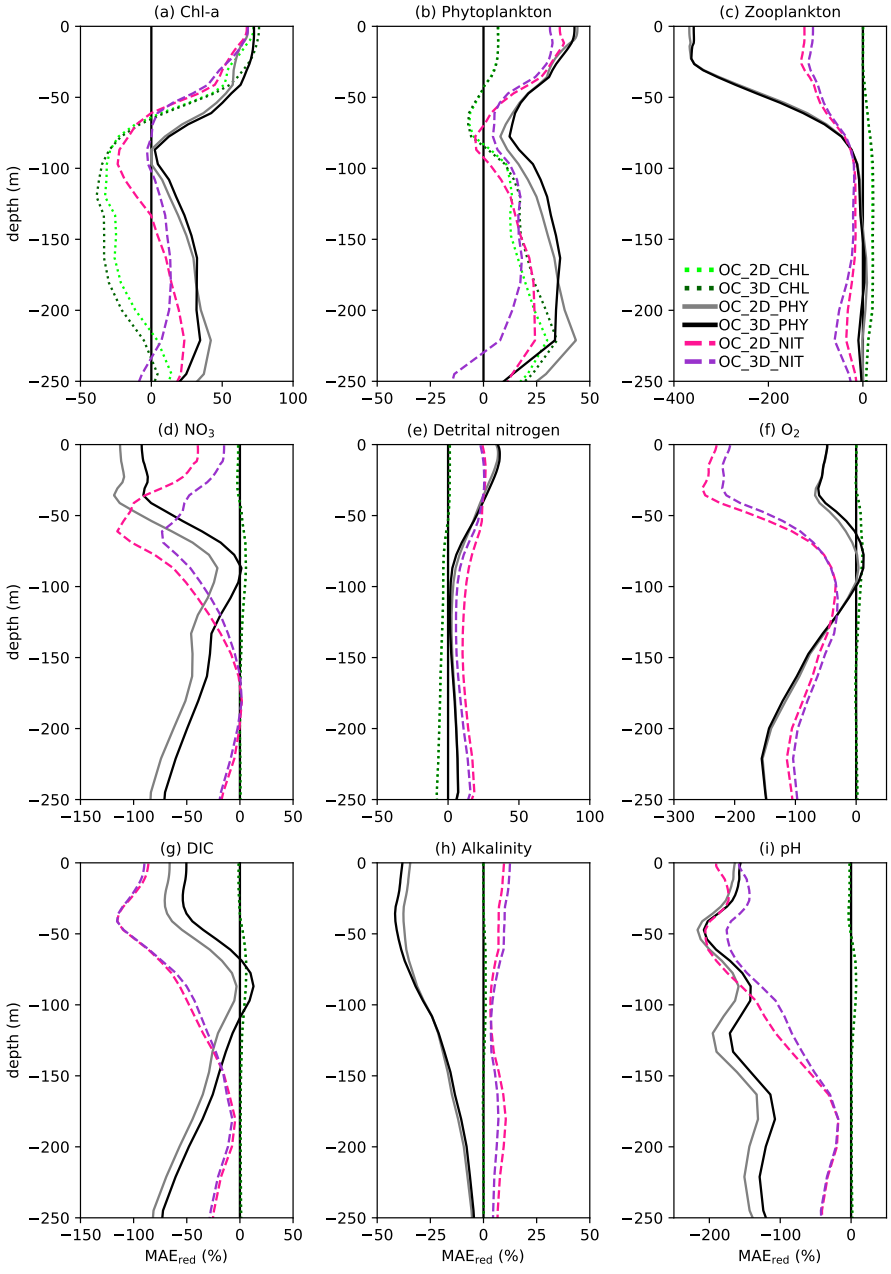

Figure 3. Global MAE_{red} over FREE for ocean colour experiments.

which are difficult to validate due to the sparsity of in situ observations, and this should be accounted for when considering the potential impact of BGC-Argo on such reanalyses. The most commonly used method is to update the phytoplankton biomass to preserve stoichiometry (Teruzzi et al., 2014; Skákala et al., 2018). Since using the Hemmings et al. (2008) balancing scheme

https://doi.org/10.5194/bg-2020-152
Preprint. Discussion started: 15 May 2020

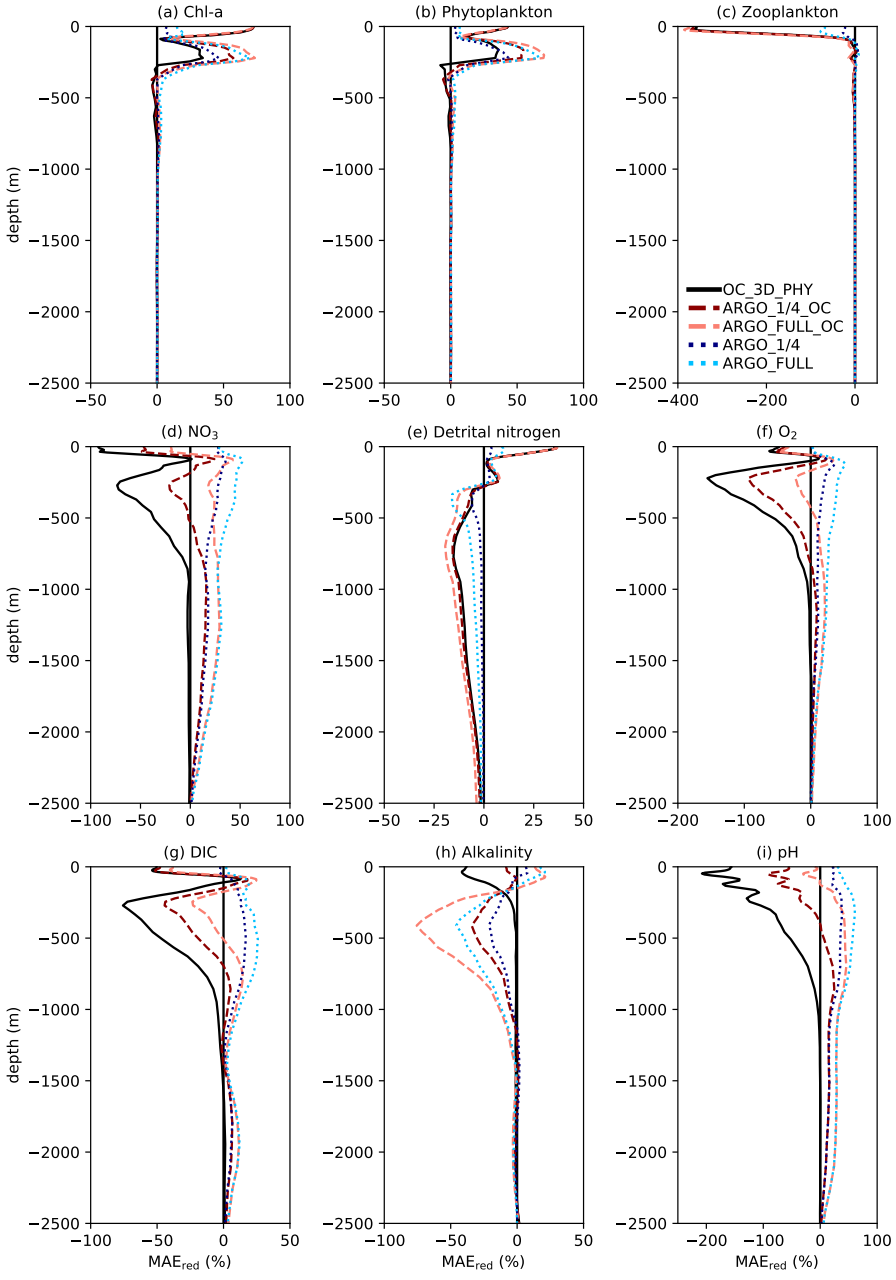

Figure 4. Global MAE_{red} over FREE for BGC-Argo experiments.

did not show a clear overall improvement in these tests, it was therefore decided to use OC_3D_PHY as the basis for OSSEs introducing the assimilation of BGC-Argo data, and to use this method when assimilating profiles of chl-a.

https://doi.org/10.5194/bg-2020-152
Preprint. Discussion started: 15 May 2020

4.3 BGC-Argo assimilation

For each of the four runs assimilating BGC-Argo data, plus OC_3D_PHY, profiles of global MAE_{red} over FREE for December 2009 are plotted in Fig. 4. Profiles are plotted for the upper 2500 m, with chl-a, NO_3, O_2, and pH observations having been produced for the upper 2000 m.

For chl-a, OC_3D_PHY, ARGO_1/4_OC, and ARGO_FULL_OC all have an MAE_{red} value of 72 % at the surface, suggesting that BGC-Argo is unable to add much information to that gained from the much denser ocean colour chl-a observations, at least at the global scale. When only BGC-Argo is assimilated, ARGO_1/4 and ARGO_FULL result in a small improvement at the surface of 7 % and 15 % respectively. Beneath the surface, at depths likely to see a deep chlorophyll maximum, BGC-Argo has much greater impact, with all four runs outperforming OC_3D_PHY. ARGO_FULL outperforms ARGO_1/4, demonstrating benefit from extra in situ observations. Combining BGC-Argo and ocean colour gives better results at this depth in ARGO_1/4_OC (which is the proposed observing system), but ARGO_FULL and ARGO_FULL_OC perform similarly. Beneath the euphotic zone, where chl-a is near-zero, the assimilation has little impact.

The results for phytoplankton biomass are very similar as for chl-a. For zooplankton biomass, the large surface degradation in OC_3D_PHY is still present in ARGO_1/4_OC and ARGO_FULL_OC, and much reduced in ARGO_1/4 and ARGO_FULL. Detrital nitrogen is improved in the upper 260–280 m in all runs, and degraded beneath that depth. Including ocean colour assimilation increases the magnitude of both the improvement and degradation, as does increasing the number of BGC-Argo floats.

For NO_3 and O_2, which are assimilated from the BGC-Argo floats, there is a clear improvement throughout the water column to 2500 m in ARGO_1/4 and ARGO_FULL, with greater improvement when more floats are assimilated. Maximum MAE_{red} is seen at 100–120 m depth, with less impact at the surface, particularly for O_2. In OC_3D_PHY, NO_3 and O_2 are degraded throughout the water column. Adding BGC-Argo to ocean colour assimilation partially mitigates this, with positive MAE_{red} at some depths and negative MAE_{red} at others.

With the carbon cycle, throughout most of the water column ARGO_1/4 and ARGO_FULL improve DIC and degrade alkalinity, with an overall improvement in the assimilated variable pH. Including ocean colour assimilation reduces the impact of BGC-Argo, and results in a degradation in pH in the surface layers.

Spatial maps of surface MAE_{red} over FREE for December 2009 for the same five runs are plotted for chl-a in Fig. 5, NO_3 in Fig. 6, and pCO_2 in Fig. 7. In OC_3D_PHY surface chl-a is almost universally improved, apart from a few small areas in the Atlantic, North Pacific, and Indian Ocean. These correspond to areas where NATURE and FREE are almost identical, as seen in Fig. 2b. As suggested in Section 4.1, it is likely that compensating errors have been introduced in FREE, which the assimilation is not fully able to address. Very little difference is made by adding BGC-Argo to ocean colour assimilation, while assimilating just BGC-Argo data gives mixed results for chl-a at the surface. In the Pacific Ocean, chl-a is slightly improved in ARGO_1/4 and further improved in ARGO_FULL, while in the Atlantic and Indian Oceans a degradation is seen. This again corresponds to regions where there is little absolute difference between NATURE and FREE (Fig. 2b).

https://doi.org/10.5194/bg-2020-152
Preprint. Discussion started: 15 May 2020

Biogeosciences
Discussions
Open Access
EGU

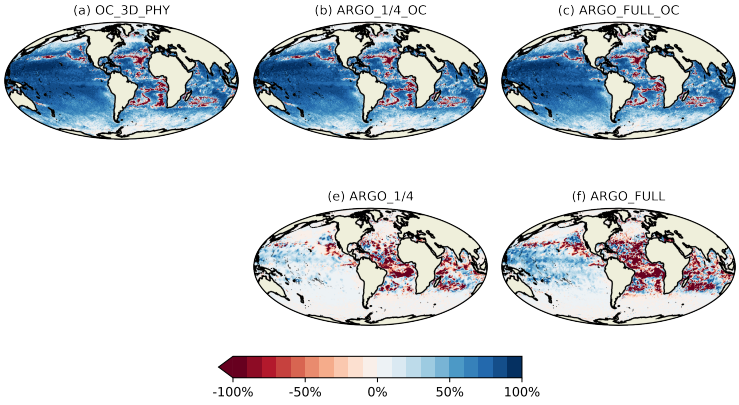

Figure 5. Surface MAE_{red} over FREE for chl-a for December 2009.

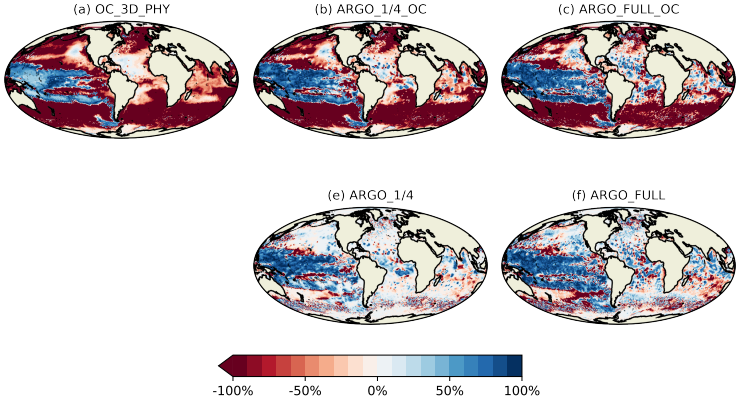

Figure 6. Surface MAE_{red} over FREE for NO_3 for December 2009.

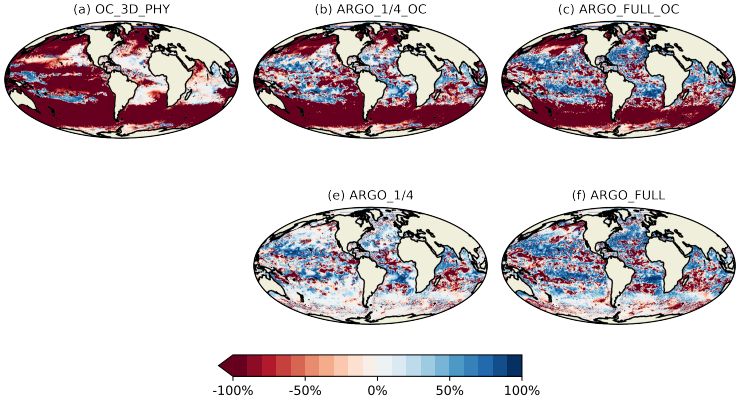

Figure 7. Surface MAE_{red} over FREE for pCO_2 for December 2009.

https://doi.org/10.5194/bg-2020-152
Preprint. Discussion started: 15 May 2020

Biogeosciences
Discussions
Open Access
EGU

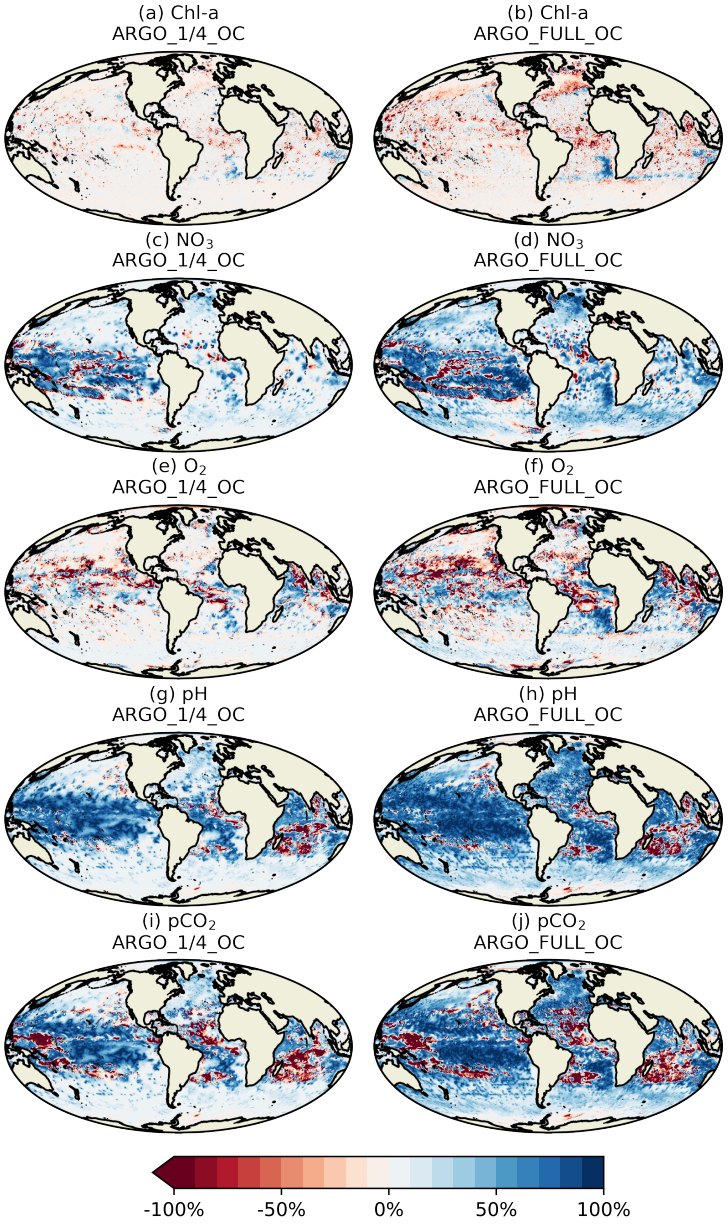

Figure 8. Surface MAE_{red} over OC_3D_PHY for chl-a, NO_3, O_2, pH, pCO_2 for December 2009.

At the surface, NO_3 is degraded almost everywhere in OC_3D_PHY (Fig. 6a), apart from the Tropical Pacific, which is where some of the largest differences are seen between NATURE and FREE (Fig. 2d). Adding BGC-Argo assimilation increases this improvement and starts to reverse the degradation in other regions, particularly in ARGO_FULL_OC. Assimilating just BGC-Argo improves NO_3 in most areas, with more impact seen with more floats, but the results are very patchy.

https://doi.org/10.5194/bg-2020-152
Preprint. Discussion started: 15 May 2020

Biogeosciences
Discussions
Open Access
EGU

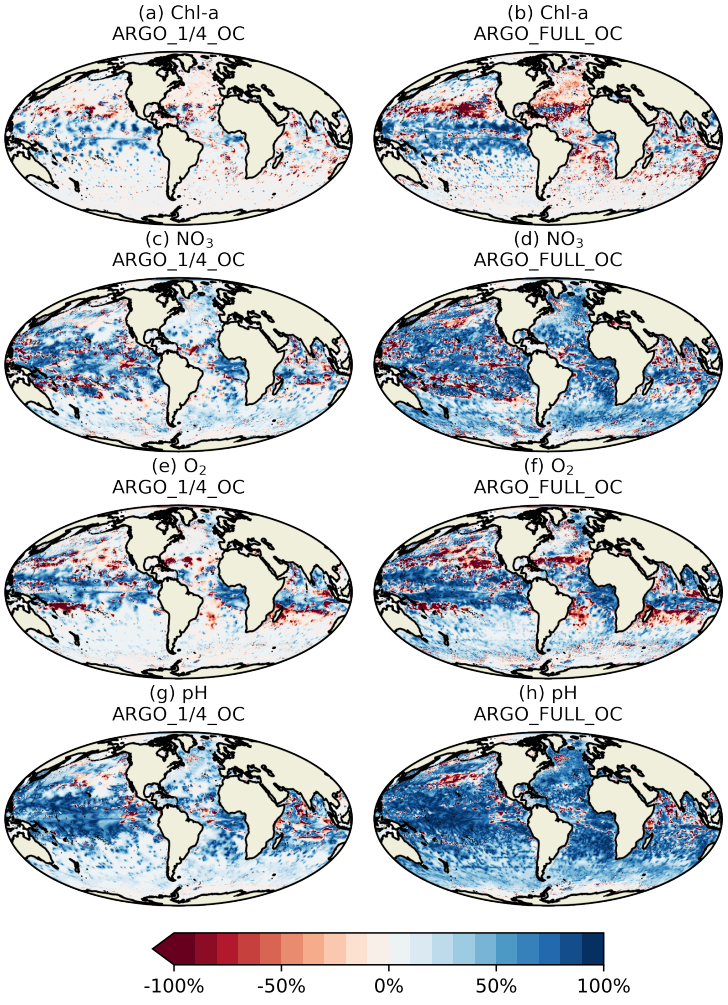

Figure 9. MAE_{red} over OC_3D_PHY for chl-a, NO_3, O_2, pH for December 2009 at 100 m depth.

The story for pCO_2 (Fig. 7) is very similar as for NO_3, but with a greater degradation introduced by ocean colour assimilation, and a greater improvement brought about by BGC-Argo assimilation. While pCO_2 is not directly assimilated, improvements to DIC and alkalinity when assimilating pH should also improve pCO_2.

Current start-of-the-art reanalyses typically assimilate ocean colour data (Fennel et al., 2019), so to demonstrate the additional impact BGC-Argo might have in these systems spatial plots of surface MAE_{red} over OC_3D_PHY are shown in Fig. 8 for the assimilated variables and pCO_2. Clear benefit is seen for surface NO_3, pH, and pCO_2, with widespread positive MAE_{red} values, especially for ARGO_FULL_OC. For O_2 the situation is more mixed, while for chl-a a small degradation is seen.

https://doi.org/10.5194/bg-2020-152
Preprint. Discussion started: 15 May 2020

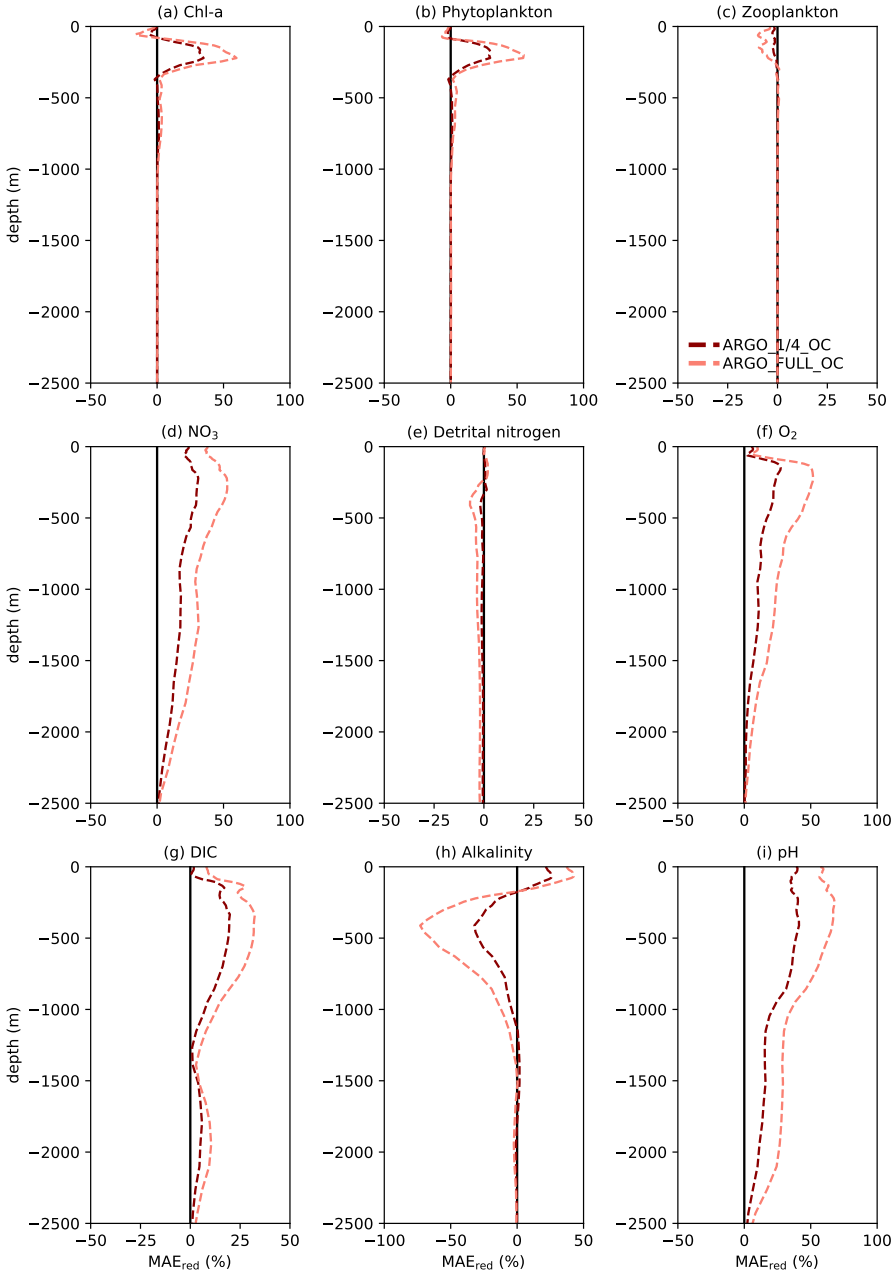

Figure 10. Global MAE_{red} over OC_3D_PHY for BGC-Argo experiments.

Beneath the surface there is greater benefit for most of the assimilated variables, as seen in the global maps of MAE_{red} over OC_3D_PHY at 100 m depth in Fig. 9. The improvement is largest for pH and smallest for chl-a, and in all cases a greater impact is seen in ARGO_FULL_OC than ARGO_1/4_OC.

https://doi.org/10.5194/bg-2020-152
Preprint. Discussion started: 15 May 2020

475 This is further demonstrated in the profiles of MAE_{red} over OC_PHY_3D plotted in Fig. 10. Apart from a small degradation in zooplankton above 250 m, detrital nitrogen below 250–350 m, and alkalinity below 175 m, all variables are improved throughout the water column. The degradation in alkalinity is compensated for by the improvement in DIC, with an overall improvement in pH. For all variables, a greater impact is seen in ARGO_FULL_OC than ARGO_1/4_OC.

5 Summary and discussion

480 A set of observing system simulation experiments (OSSEs) has been performed to explore the impact on global ocean biogeochemical reanalyses of assimilating currently-available ocean colour data, and assess the potential impact of assimilating BGC-Argo data. Two different potential BGC-Argo array distributions were tested: one where biogeochemical sensors are placed on all current Argo floats, and one where biogeochemical sensors are placed on a quarter of current Argo floats. This latter approximately corresponds to the proposed BGC-Argo array of 1000 floats (Roemmich et al., 2019). Three different
485 strategies for updating model variables when assimilating ocean colour were assessed: all similarly improved the assimilated variable surface chl-a, but had a mixed impact on the wider ecosystem and carbon cycle. Assimilating BGC-Argo data gave no added benefit over ocean colour in terms of simulating surface chl-a, but for most other variables, including sub-surface chl-a, adding BGC-Argo improved results throughout the water column. This included surface pCO_2, which was not assimilated but is an important output of reanalyses. Both BGC-Argo array distributions gave benefits, with greater improvements seen with
490 increased numbers of observations.

Real-world experiments assimilating chl-a from ocean colour have widely found benefits when validating surface chl-a against independent observations (Gehlen et al., 2015; Fennel et al., 2019), a conclusion echoed in this study. The impact of ocean colour assimilation on the wider model state has always been more ambiguous, with various studies reporting largely neutral or sometimes negative results, with some evidence of positive impacts highlighted (e.g. Gregg, 2008; Ciavatta et al.,
495 2011; Fontana et al., 2013; Ford and Barciela, 2017). The sparsity of in situ observations, especially for variables such as phytoplankton and zooplankton biomass, has always made it difficult to validate results, or compare conclusions from different studies. Many studies have used inherently multivariate assimilation methods such as the ensemble Kalman filter (Evensen, 2003), while others have employed balance relationships (Ford et al., 2012; Rousseaux and Gregg, 2012; Teruzzi et al., 2014; Skákala et al., 2018). This study tested three variations of the latter: just updating chl-a, also updating phytoplankton biomass,
500 and the nitrogen balancing scheme of Hemmings et al. (2008). Solely updating chl-a essentially just acted to change the phytoplankton carbon-to-chlorophyll ratio. This improved chl-a and slightly improved phytoplankton biomass, but had minimal impact on the wider model state. While no damage was done, it was unable to fulfil the ambition of extracting maximum information from the assimilated data. Updating phytoplankton biomass, a simple extra step which improved phytoplankton biomass itself and so should be expected to improve other model variables, resulted in a degradation of all other variables
505 examined except for detritus. Zooplankton biomass was especially affected. It seems likely that this degradation occurred due to the changed MEDUSA parameter settings between NATURE and FREE, meaning that the underlying processes were altered such that identical concentrations of phytoplankton now led to different concentrations of other variables. This suggests that

https://doi.org/10.5194/bg-2020-152
Preprint. Discussion started: 15 May 2020

unless a given biogeochemical model can accurately describe all relevant biogeochemical processes in the ocean, which has not yet been demonstrated, simply improving phytoplankton concentrations might be as likely to degrade as improve other variables. This will also be the case for assimilation schemes which use ensembles to generate cross-correlations between chl-a and other model variables. Using the nitrogen balancing scheme of Hemmings et al. (2008), which explicitly updates several model state variables to try and account for differing errors in growth and loss processes, generally gave an improvement over just updating phytoplankton biomass, but resulted in further degradation of some variables. Such a scheme offers more potential for controlling the wider biogeochemical state, especially if it could be expanded to alter parameter values as well as state variables. Furthermore, it was designed for use with the simpler HadOCC model (Palmer and Totterdell, 2001), with which it has been successfully demonstrated (Hemmings et al., 2008; Ford et al., 2012), and only minimally altered for use with MEDUSA, so more specific tuning may help.

Adding assimilation of BGC-Argo profiles of chl-a, NO_3, O_2, and pH brought clear improvements to all assimilated variables, and some unassimilated ones. The impact was increased with a larger BGC-Argo array, suggesting that benefits may be seen up to and beyond the target array size of 1000 floats. The observations added important sub-surface information which cannot be obtained from satellite data, but which can yield improvements in simulations of variables such as air-sea CO_2 fluxes. Where BGC-Argo data did not result in improvements was for surface chl-a and O_2. For chl-a, ocean colour observations were able to provide this information, while for O_2 and other variables in situ observing technologies such as gliders may be able to play a role (Telszewski et al., 2018). It should be noted though that the OSSE framework used here did not consider possible real-world issues such as observation biases and inconsistencies between ocean colour and BGC-Argo chl-a observations.

From the point of view of ocean data assimilation, the development of BGC-Argo will bring significant advances in reanalysis and forecasting skill. The proposed array of 1000 floats will be enough to deliver clear improvements, but a larger array would be likely to bring further benefits still. Ocean colour and BGC-Argo provide complementary information, so maintaining and developing the existing ocean colour satellite constellation should also be a priority. Technologies such as gliders may also bring additional benefits, especially for nutrients and oxygen in the mixed layer.

There is also much scope for improving data assimilation methodologies to better use existing satellite data, and sparse in situ observations, which could bring at least as much benefit as expanding observing systems. Multivariate balancing, and better integration with physics data assimilation, may help improve unassimilated variables. More effective ways of spreading information from sparse data, such as cross-covariances based on empirical orthogonal functions or derived from an ensemble assimilation scheme, should also be considered.

Data availability. The nature of the 4D data generated in running the model experiments requires a large tape storage facility. These data are in excess of 100 terabytes (TB). However, the data can be made available upon request from the author.

Author contributions. DF set up and performed the experiments, analysed the results, and wrote the manuscript.

https://doi.org/10.5194/bg-2020-152
Preprint. Discussion started: 15 May 2020

Biogeosciences Discussions Open Access EGU

Competing interests. The author declares that they have no conflict of interest.

Acknowledgements. This study received funding from the European Union's Horizon 2020 Research and Innovation program under Grant Agreement 633211 (AtlantOS). The author would like to thank Susan Kay and Matt Martin for useful discussions and comments on the draft manuscript.

https://doi.org/10.5194/bg-2020-152
Preprint. Discussion started: 15 May 2020

References

Altieri, A. H. and Gedan, K. B.: Climate change and dead zones, Global Change Biology, 21, 1395–1406, https://doi.org/10.1111/gcb.12754, https://onlinelibrary.wiley.com/doi/abs/10.1111/gcb.12754, 2015.

Anderson, L. A., Robinson, A. R., and Lozano, C. J.: Physical and biological modeling in the Gulf Stream region:: I. Data assimilation methodology, Deep Sea Research Part I: Oceanographic Research Papers, 47, 1787 – 1827, https://doi.org/https://doi.org/10.1016/S0967-0637(00)00019-4, http://www.sciencedirect.com/science/article/pii/S0967063700000194, 2000.

Arnold, C. P. and Dey, C. H.: Observing-Systems Simulation Experiments: Past, Present, and Future, Bulletin of the American Meteorological Society, 67, 687–695, https://doi.org/10.1175/1520-0477(1986)067<0687:OSSEPP>2.0.CO;2, https://doi.org/10.1175/1520-0477(1986)067<0687:OSSEPP>2.0.CO;2, 1986.

Bannister, R. N.: A review of forecast error covariance statistics in atmospheric variational data assimilation. I: Characteristics and measurements of forecast error covariances, Quarterly Journal of the Royal Meteorological Society, 134, 1951–1970, https://doi.org/10.1002/qj.339, https://rmets.onlinelibrary.wiley.com/doi/abs/10.1002/qj.339, 2008.

Bates, N. R., Astor, Y. M., Church, M. J., Currie, K., Dore, J. E., González-Dávila, M., Lorenzoni, L., Muller-Karger, F., Olafsson, J., and Santana-Casiano, J. M.: A Time-Series View of Changing Surface Ocean Chemistry Due to Ocean Uptake of Anthropogenic CO_2 and Ocean Acidification, Oceanography, 27, 126–141, http://www.jstor.org/stable/24862128, 2014.

Behrenfeld, M. J. and Boss, E. S.: Resurrecting the Ecological Underpinnings of Ocean Plankton Blooms, Annual Review of Marine Science, 6, 167–194, https://doi.org/10.1146/annurev-marine-052913-021325, https://doi.org/10.1146/annurev-marine-052913-021325, pMID: 24079309, 2014.

Biogeochemical-Argo Planning Group: The scientific rationale, design and Implementation Plan for a Biogeochemical-Argo float array, Edited by Ken Johnson and Hervé Claustre, https://doi.org/10.13155/46601, 2016.

Blockley, E. W., Martin, M. J., McLaren, A. J., Ryan, A. G., Waters, J., Lea, D. J., Mirouze, I., Peterson, K. A., Sellar, A., and Storkey, D.: Recent development of the Met Office operational ocean forecasting system: an overview and assessment of the new Global FOAM forecasts, Geoscientific Model Development, 7, 2613–2638, https://doi.org/10.5194/gmd-7-2613-2014, https://www.geosci-model-dev.net/7/2613/2014/, 2014.

Bloom, S. C., Takacs, L. L., da Silva, A. M., and Ledvina, D.: Data Assimilation Using Incremental Analysis Updates, Monthly Weather Review, 124, 1256–1271, https://doi.org/10.1175/1520-0493(1996)124<1256:DAUIAU>2.0.CO;2, https://doi.org/10.1175/1520-0493(1996)124<1256:DAUIAU>2.0.CO;2, 1996.

Boss, E., Swift, D., Taylor, L., Brickley, P., Zaneveld, R., Riser, S., Perry, M. J., and Strutton, P. G.: Observations of pigment and particle distributions in the western North Atlantic from an autonomous float and ocean color satellite, Limnology and Oceanography, 53, 2112–2122, https://doi.org/10.4319/lo.2008.53.5_part_2.2112, https://aslopubs.onlinelibrary.wiley.com/doi/abs/10.4319/lo.2008.53.5_part_2.2112, 2008.

Calvert, D. and Siddorn, J.: Revised vertical mixing parameters for the UK community standard configuration of the global NEMO ocean model, Met Office Hadley Centre Technical Note, 95, https://library.metoffice.gov.uk/Portal/Default/en-GB/RecordView/Index/207517, 2013.

Campbell, J. W.: The lognormal distribution as a model for bio-optical variability in the sea, Journal of Geophysical Research: Oceans, 100, 13 237–13 254, https://doi.org/10.1029/95JC00458, https://agupubs.onlinelibrary.wiley.com/doi/abs/10.1029/95JC00458, 1995.

Ciavatta, S., Torres, R., Saux-Picart, S., and Allen, J. I.: Can ocean color assimilation improve biogeochemical hindcasts in shelf seas?, Journal of Geophysical Research: Oceans, 116, https://doi.org/10.1029/2011JC007219, https://agupubs.onlinelibrary.wiley.com/doi/abs/10.1029/2011JC007219, 2011.

Ciavatta, S., Kay, S., Saux-Picart, S., Butenschön, M., and Allen, J. I.: Decadal reanalysis of biogeochemical indicators and fluxes in the North West European shelf-sea ecosystem, Journal of Geophysical Research: Oceans, 121, 1824–1845, https://doi.org/10.1002/2015JC011496, https://agupubs.onlinelibrary.wiley.com/doi/abs/10.1002/2015JC011496, 2016.

Cossarini, G., Mariotti, L., Feudale, L., Mignot, A., Salon, S., Taillandier, V., Teruzzi, A., and D'Ortenzio, F.: Towards operational 3D-Var assimilation of chlorophyll Biogeochemical-Argo float data into a biogeochemical model of the Mediterranean Sea, Ocean Modelling, 133, 112 – 128, https://doi.org/https://doi.org/10.1016/j.ocemod.2018.11.005, http://www.sciencedirect.com/science/article/pii/S146350031830060X, 2019.

Davidson, F., Alvera-Azcárate, A., Barth, A., Brassington, G. B., Chassignet, E. P., Clementi, E., De Mey-Frémaux, P., Divakaran, P., Harris, C., Hernandez, F., Hogan, P., Hole, L. R., Holt, J., Liu, G., Lu, Y., Lorente, P., Maksymczuk, J., Martin, M., Mehra, A., Melsom, A., Mo, H., Moore, A., Oddo, P., Pascual, A., Pequignet, A.-C., Kourafalou, V., Ryan, A., Siddorn, J., Smith, G., Spindler, D., Spindler, T., Stanev, E. V., Staneva, J., Storto, A., Tanajura, C., Vinayachandran, P. N., Wan, L., Wang, H., Zhang, Y., Zhu, X., and Zu, Z.: Synergies in Operational Oceanography: The Intrinsic Need for Sustained Ocean Observations, Frontiers in Marine Science, 6, 450, https://doi.org/10.3389/fmars.2019.00450, https://www.frontiersin.org/article/10.3389/fmars.2019.00450, 2019.

Dee, D. P., Uppala, S. M., Simmons, A. J., Berrisford, P., Poli, P., Kobayashi, S., Andrae, U., Balmaseda, M. A., Balsamo, G., Bauer, P., Bechtold, P., Beljaars, A. C. M., van de Berg, L., Bidlot, J., Bormann, N., Delsol, C., Dragani, R., Fuentes, M., Geer, A. J., Haimberger, L., Healy, S. B., Hersbach, H., Hólm, E. V., Isaksen, L., Kållberg, P., Köhler, M., Matricardi, M., McNally, A. P., Monge-Sanz, B. M., Morcrette, J.-J., Park, B.-K., Peubey, C., de Rosnay, P., Tavolato, C., Thépaut, J.-N., and Vitart, F.: The ERA-Interim reanalysis: configuration and performance of the data assimilation system, Quarterly Journal of the Royal Meteorological Society, 137, 553–597, https://doi.org/10.1002/qj.828, https://rmets.onlinelibrary.wiley.com/doi/abs/10.1002/qj.828, 2011.

Diaz, R. J. and Rosenberg, R.: Spreading Dead Zones and Consequences for Marine Ecosystems, Science, 321, 926–929, https://doi.org/10.1126/science.1156401, https://science.sciencemag.org/content/321/5891/926, 2008.

Doney, S. C., Fabry, V. J., Feely, R. A., and Kleypas, J. A.: Ocean Acidification: The Other CO_2 Problem, Annual Review of Marine Science, 1, 169–192, https://doi.org/10.1146/annurev.marine.010908.163834, https://doi.org/10.1146/annurev.marine.010908.163834, pMID: 21141034, 2009.

Evensen, G.: The ensemble Kalman filter: Theoretical formulation and practical implementation, Ocean Dynamics, 53, 343–367, https://doi.org/10.1007/s10236-003-0036-9, 2003.

Eyring, V., Bony, S., Meehl, G. A., Senior, C. A., Stevens, B., Stouffer, R. J., and Taylor, K. E.: Overview of the Coupled Model Intercomparison Project Phase 6 (CMIP6) experimental design and organization, Geoscientific Model Development, 9, 1937–1958, https://doi.org/10.5194/gmd-9-1937-2016, https://www.geosci-model-dev.net/9/1937/2016/, 2016.

FAO: The State of World Fisheries and Aquaculture 2016. Contributing to food security and nutrition for all, Rome, 2016.

Fennel, K., Gehlen, M., Brasseur, P., Brown, C. W., Ciavatta, S., Cossarini, G., Crise, A., Edwards, C. A., Ford, D., Friedrichs, M. A. M., Gregoire, M., Jones, E., Kim, H.-C., Lamouroux, J., Murtugudde, R., Perruche, C., and the GODAE OceanView Marine Ecosystem Analysis and Prediction Task Team: Advancing Marine Biogeochemical and Ecosystem Reanalyses and Forecasts as Tools for Monitoring and Managing Ecosystem Health, Frontiers in Marine Science, 6, 89, https://doi.org/10.3389/fmars.2019.00089, https://www.frontiersin.org/article/10.3389/fmars.2019.00089, 2019.

https://doi.org/10.5194/bg-2020-152
Preprint. Discussion started: 15 May 2020

Fontana, C., Brasseur, P., and Brankart, J.-M.: Toward a multivariate reanalysis of the North Atlantic Ocean biogeochemistry during 1998–2006 based on the assimilation of SeaWiFS chlorophyll data, Ocean Science, 9, 37–56, https://doi.org/10.5194/os-9-37-2013, https://www.ocean-sci.net/9/37/2013/, 2013.

Ford, D.: Assessing the role and consistency of satellite observation products in global physical-biogeochemical ocean reanalysis, Ocean Science Discussions, 2019, 1–25, https://doi.org/10.5194/os-2019-118, https://www.ocean-sci-discuss.net/os-2019-118/, 2019.

Ford, D. and Barciela, R.: Global marine biogeochemical reanalyses assimilating two different sets of merged ocean colour products, Remote Sensing of Environment, 203, 40 – 54, https://doi.org/https://doi.org/10.1016/j.rse.2017.03.040, http://www.sciencedirect.com/science/article/pii/S0034425717301438, earth Observation of Essential Climate Variables, 2017.

Ford, D. A., Edwards, K. P., Lea, D., Barciela, R. M., Martin, M. J., and Demaria, J.: Assimilating GlobColour ocean colour data into a pre-operational physical-biogeochemical model, Ocean Science, 8, 751–771, https://doi.org/10.5194/os-8-751-2012, https://www.ocean-sci.net/8/751/2012/, 2012.

Fujii, Y., Rémy, E., Zuo, H., Oke, P., Halliwell, G., Gasparin, F., Benkiran, M., Loose, N., Cummings, J., Xie, J., Xue, Y., Masuda, S., Smith, G. C., Balmaseda, M., Germineaud, C., Lea, D. J., Larnicol, G., Bertino, L., Bonaduce, A., Brasseur, P., Donlon, C., Heimbach, P., Kim, Y., Kourafalou, V., Le Traon, P.-Y., Martin, M., Paturi, S., Tranchant, B., and Usui, N.: Observing System Evaluation Based on Ocean Data Assimilation and Prediction Systems: On-Going Challenges and a Future Vision for Designing and Supporting Ocean Observational Networks, Frontiers in Marine Science, 6, 417, https://doi.org/10.3389/fmars.2019.00417, https://www.frontiersin.org/article/10.3389/fmars.2019.00417, 2019.

Garcia, H. E., Weathers, K., Paver, C. R., Smolyar, I., Boyer, T. P., Locarnini, R. A., Zweng, M. M., Mishonov, A. V., Baranova, O. K., Seidov, D., and Reagan, J. R.: World Ocean Atlas 2018, Volume 4: Dissolved Inorganic Nutrients (phosphate, nitrate and nitrate+nitrite, silicate), A. Mishonov Technical Ed.; NOAA Atlas NESDIS 84, 2018.

Gasparin, F., Guinehut, S., Mao, C., Mirouze, I., Rémy, E., King, R. R., Hamon, M., Reid, R., Storto, A., Le Traon, P.-Y., Martin, M. J., and Masina, S.: Requirements for an Integrated in situ Atlantic Ocean Observing System From Coordinated Observing System Simulation Experiments, Frontiers in Marine Science, 6, 83, https://doi.org/10.3389/fmars.2019.00083, https://www.frontiersin.org/article/10.3389/fmars.2019.00083, 2019.

Gehlen, M., Barciela, R., Bertino, L., Brasseur, P., Butenschön, M., Chai, F., Crise, A., Drillet, Y., Ford, D., Lavoie, D., Lehodey, P., Perruche, C., Samuelsen, A., and Simon, E.: Building the capacity for forecasting marine biogeochemistry and ecosystems: recent advances and future developments, Journal of Operational Oceanography, 8, s168–s187, https://doi.org/10.1080/1755876X.2015.1022350, https://doi.org/10.1080/1755876X.2015.1022350, 2015.

Germineaud, C., Brankart, J.-M., and Brasseur, P.: An Ensemble-Based Probabilistic Score Approach to Compare Observation Scenarios: An Application to Biogeochemical-Argo Deployments, Journal of Atmospheric and Oceanic Technology, 36, 2307–2326, https://doi.org/10.1175/JTECH-D-19-0002.1, https://doi.org/10.1175/JTECH-D-19-0002.1, 2019.

Gregg, W. W.: Assimilation of SeaWiFS ocean chlorophyll data into a three-dimensional global ocean model, Journal of Marine Systems, 69, 205 – 225, https://doi.org/https://doi.org/10.1016/j.jmarsys.2006.02.015, http://www.sciencedirect.com/science/article/pii/S0924796307000607, physical-Biological Interactions in the Upper Ocean, 2008.

Groom, S., Sathyendranath, S., Ban, Y., Bernard, S., Brewin, R., Brotas, V., Brockmann, C., Chauhan, P., Choi, J.-k., Chuprin, A., Ciavatta, S., Cipollini, P., Donlon, C., Franz, B., He, X., Hirata, T., Jackson, T., Kampel, M., Krasemann, H., Lavender, S., Pardo-Martinez, S., Mélin, F., Platt, T., Santoleri, R., Skákala, J., Schaeffer, B., Smith, M., Steinmetz, F., Valente, A., and Wang, M.: Satellite Ocean Colour: Current

https://doi.org/10.5194/bg-2020-152
Preprint. Discussion started: 15 May 2020

Status and Future Perspective, Frontiers in Marine Science, 6, 485, https://doi.org/10.3389/fmars.2019.00485, https://www.frontiersin.org/article/10.3389/fmars.2019.00485, 2019.

Guiavarc'h, C., Roberts-Jones, J., Harris, C., Lea, D. J., Ryan, A., and Ascione, I.: Assessment of ocean analysis and forecast from an atmosphere–ocean coupled data assimilation operational system, Ocean Science, 15, 1307–1326, https://doi.org/10.5194/os-15-1307-2019, https://www.ocean-sci.net/15/1307/2019/, 2019.

Halliwell, G. R., Srinivasan, A., Kourafalou, V., Yang, H., Willey, D., Le Hénaff, M., and Atlas, R.: Rigorous Evaluation of a Fraternal Twin Ocean OSSE System for the Open Gulf of Mexico, Journal of Atmospheric and Oceanic Technology, 31, 105–130, https://doi.org/10.1175/JTECH-D-13-00011.1, https://doi.org/10.1175/JTECH-D-13-00011.1, 2014.

Halliwell, G. R., Mehari, M. F., Hénaff, M. L., Kourafalou, V. H., Androulidakis, I. S., Kang, H. S., and Atlas, R.: North Atlantic Ocean OSSE system: Evaluation of operational ocean observing system components and supplemental seasonal observations for potentially improving tropical cyclone prediction in coupled systems, Journal of Operational Oceanography, 10, 154–175, https://doi.org/10.1080/1755876X.2017.1322770, https://doi.org/10.1080/1755876X.2017.1322770, 2017.

Hemmings, J. C. P., Barciela, R. M., and Bell, M. J.: Ocean color data assimilation with material conservation for improving model estimates of air-sea CO2 flux, Journal of Marine Research, 66, 87–126, https://doi.org/doi:10.1357/002224008784815739, https://www.ingentaconnect.com/content/jmr/jmr/2008/00000066/00000001/art00004, 2008.

Hemmings, J. C. P., Challenor, P. G., and Yool, A.: Mechanistic site-based emulation of a global ocean biogeochemical model (MEDUSA 1.0) for parametric analysis and calibration: an application of the Marine Model Optimization Testbed (MarMOT 1.1), Geoscientific Model Development, 8, 697–731, https://doi.org/10.5194/gmd-8-697-2015, https://www.geosci-model-dev.net/8/697/2015/, 2015.

Hoffman, R. N. and Atlas, R.: Future Observing System Simulation Experiments, Bulletin of the American Meteorological Society, 97, 1601–1616, https://doi.org/10.1175/BAMS-D-15-00200.1, https://doi.org/10.1175/BAMS-D-15-00200.1, 2016.

Hunke, C., E., Lipscomb, H., W., Turner, K., A., Jeffery, N., Elliott, and S.: CICE: the Los Alamos sea ice model documentation and software users' manual, Version 5.1, LA-CC-06-012, Los Alamos National Laboratory, N.M., 2015.

IPCC: Climate Change 2014: Synthesis Report. Contribution of Working Groups I, II and III to the Fifth Assessment Report of the Intergovernmental Panel on Climate Change [Core Writing Team, R.K. Pachauri and L.A. Meyer (eds.)], IPCC, Geneva, Switzerland, 2014.

Jackson, D. R., Keil, M., and Devenish, B. J.: Use of Canadian Quick covariances in the Met Office data assimilation system, Quarterly Journal of the Royal Meteorological Society, 134, 1567–1582, https://doi.org/10.1002/qj.294, https://rmets.onlinelibrary.wiley.com/doi/abs/10.1002/qj.294, 2008.

Janjić, T., Bormann, N., Bocquet, M., Carton, J. A., Cohn, S. E., Dance, S. L., Losa, S. N., Nichols, N. K., Potthast, R., Waller, J. A., and Weston, P.: On the representation error in data assimilation, Quarterly Journal of the Royal Meteorological Society, 144, 1257–1278, https://doi.org/10.1002/qj.3130, https://rmets.onlinelibrary.wiley.com/doi/abs/10.1002/qj.3130, 2018.

Johnson, K. S., Plant, J. N., Coletti, L. J., Jannasch, H. W., Sakamoto, C. M., Riser, S. C., Swift, D. D., Williams, N. L., Boss, E., Haëntjens, N., Talley, L. D., and Sarmiento, J. L.: Biogeochemical sensor performance in the SOCCOM profiling float array, Journal of Geophysical Research: Oceans, 122, 6416–6436, https://doi.org/10.1002/2017JC012838, https://agupubs.onlinelibrary.wiley.com/doi/abs/10.1002/2017JC012838, 2017.

Kalnay, E.: Atmospheric modeling, data assimilation and predictability, Cambridge University Press, 2003.

Kobayashi, S., Ota, Y., Harada, Y., Ebita, A., Moriya, M., Onoda, H., Onogi, K., Kamahori, H., Kobayashi, C., Endo, H., Miyaoka, K., and Takahashi, K.: The JRA-55 Reanalysis: General Specifications and Basic Characteristics, Journal of the Meteorological Society of Japan. Ser. II, 93, 5–48, https://doi.org/10.2151/jmsj.2015-001, 2015.

https://doi.org/10.5194/bg-2020-152
Preprint. Discussion started: 15 May 2020

Kwiatkowski, L., Yool, A., Allen, J. I., Anderson, T. R., Barciela, R., Buitenhuis, E. T., Butenschön, M., Enright, C., Halloran, P. R., Le Quéré, C., de Mora, L., Racault, M.-F., Sinha, B., Totterdell, I. J., and Cox, P. M.: iMarNet: an ocean biogeochemistry model intercomparison project within a common physical ocean modelling framework, Biogeosciences, 11, 7291–7304, https://doi.org/10.5194/bg-11-7291-2014, https://www.biogeosciences.net/11/7291/2014/, 2014.

Landschützer, P., Gruber, N., and Bakker, D. C. E.: A 30 years observation-based global monthly gridded sea surface pCO_2 product from 1982 through 2011 (NCEI Accession 0160558), https://doi.org/10.3334/cdiac/otg.spco2_1982_2011_eth_somffn, 2015a.

Landschützer, P., Gruber, N., Haumann, F. A., Rödenbeck, C., Bakker, D. C. E., van Heuven, S., Hoppema, M., Metzl, N., Sweeney, C., Takahashi, T., Tilbrook, B., and Wanninkhof, R.: The reinvigoration of the Southern Ocean carbon sink, Science, 349, 1221–1224, https://doi.org/10.1126/science.aab2620, https://science.sciencemag.org/content/349/6253/1221, 2015b.

Lévy, M., Estublier, A., and Madec, G.: Choice of an advection scheme for biogeochemical models, Geophysical Research Letters, 28, 3725–3728, https://doi.org/10.1029/2001GL012947, https://agupubs.onlinelibrary.wiley.com/doi/abs/10.1029/2001GL012947, 2001.

Lindstrom, E., Gunn, J., Fischer, A., McCurdy, A., and Glover, L.: A Framework for Ocean Observing. By the Task Team for an Integrated Framework for Sustained Ocean Observing, UNESCO 2012, IOC/INF-1284, https://doi.org/10.5270/OceanObs09-FOO, 2012.

MacLachlan, C., Arribas, A., Peterson, K. A., Maidens, A., Fereday, D., Scaife, A. A., Gordon, M., Vellinga, M., Williams, A., Comer, R. E., Camp, J., Xavier, P., and Madec, G.: Global Seasonal forecast system version 5 (GloSea5): a high-resolution seasonal forecast system, Quarterly Journal of the Royal Meteorological Society, 141, 1072–1084, https://doi.org/10.1002/qj.2396, https://rmets.onlinelibrary.wiley.com/doi/abs/10.1002/qj.2396, 2015.

Madec, G.: NEMO ocean engine, Note du Pole de modélisation, Institut Pierre-Simon Laplace (IPSL), France, No 27 ISSN No, 1288-1619, 2008.

Mao, C., King, R. R., Reid, R., Martin, M., and Good, S.: Impact of in situ Observations in FOAM: An Observing System Simulation Experiments Perspective, in prep.

Martin, G. M., Milton, S. F., Senior, C. A., Brooks, M. E., Ineson, S., Reichler, T., and Kim, J.: Analysis and Reduction of Systematic Errors through a Seamless Approach to Modeling Weather and Climate, Journal of Climate, 23, 5933–5957, https://doi.org/10.1175/2010JCLI3541.1, https://doi.org/10.1175/2010JCLI3541.1, 2010.

Masutani, M., Schlatter, T. W., Errico, R. M., Stoffelen, A., Andersson, E., Lahoz, W., Woollen, J. S., Emmitt, G. D., Riishøjgaard, L.-P., and Lord, S. J.: Observing System Simulation Experiments, in: Data Assimilation: Making Sense of Observations, edited by Lahoz, W., Khattatov, B., and Menard, R., pp. 647–679, Springer Berlin Heidelberg, Berlin, Heidelberg, https://doi.org/10.1007/978-3-540-74703-1_24, https://doi.org/10.1007/978-3-540-74703-1_24, 2010.

McKinley, G. A., Fay, A. R., Lovenduski, N. S., and Pilcher, D. J.: Natural Variability and Anthropogenic Trends in the Ocean Carbon Sink, Annual Review of Marine Science, 9, 125–150, https://doi.org/10.1146/annurev-marine-010816-060529, https://doi.org/10.1146/annurev-marine-010816-060529, pMID: 27620831, 2017.

Mirouze, I., Blockley, E. W., Lea, D. J., Martin, M. J., and Bell, M. J.: A multiple length scale correlation operator for ocean data assimilation, Tellus A: Dynamic Meteorology and Oceanography, 68, 29 744, https://doi.org/10.3402/tellusa.v68.29744, https://doi.org/10.3402/tellusa.v68.29744, 2016.

Mogensen, K. S., Balmaseda, M. A., Weaver, A., Martin, M., and Vidard, A.: NEMOVAR: a variational data assimilation system for the NEMO ocean model, ECMWF Newsletter, 120, 17–21, https://doi.org/10.21957/3yj3mh16iq, https://www.ecmwf.int/node/17483, 2009.

Mogensen, K. S., Balmaseda, M. A., and Weaver, A.: The NEMOVAR ocean data assimilation system as implemented in the ECMWF ocean analysis for System 4, Tech. Rep. 668, ECMWF, https://doi.org/10.21957/x5y9yrtm, https://www.ecmwf.int/node/11174, 2012.

https://doi.org/10.5194/bg-2020-152
Preprint. Discussion started: 15 May 2020

Munhoven, G.: Mathematics of the total alkalinity-pH equation - pathway to robust and universal solution algorithms: the SolveSAPHE package v1.0.1, Geoscientific Model Development, 6, 1367–1388, https://doi.org/10.5194/gmd-6-1367-2013, https://www.geosci-model-dev.net/6/1367/2013/, 2013.

Orr, J. C. and Epitalon, J.-M.: Improved routines to model the ocean carbonate system: mocsy 2.0, Geoscientific Model Development, 8, 485–499, https://doi.org/10.5194/gmd-8-485-2015, https://www.geosci-model-dev.net/8/485/2015/, 2015.

Palmer, J. and Totterdell, I.: Production and export in a global ocean ecosystem model, Deep Sea Research Part I: Oceanographic Research Papers, 48, 1169 – 1198, https://doi.org/https://doi.org/10.1016/S0967-0637(00)00080-7, http://www.sciencedirect.com/science/article/pii/S0967063700000807, 2001.

Park, J.-Y., Stock, C. A., Yang, X., Dunne, J. P., Rosati, A., John, J., and Zhang, S.: Modeling Global Ocean Biogeochemistry With Physical Data Assimilation: A Pragmatic Solution to the Equatorial Instability, Journal of Advances in Modeling Earth Systems, 10, 891–906, https://doi.org/10.1002/2017MS001223, https://agupubs.onlinelibrary.wiley.com/doi/abs/10.1002/2017MS001223, 2018.

Polavarapu, S., Ren, S., Rochon, Y., Sankey, D., Ek, N., Koshyk, J., and Tarasick, D.: Data assimilation with the Canadian middle atmosphere model, Atmosphere-Ocean, 43, 77–100, https://doi.org/10.3137/ao.430105, https://doi.org/10.3137/ao.430105, 2005.

Racault, M.-F., Sathyendranath, S., Brewin, R. J. W., Raitsos, D. E., Jackson, T., and Platt, T.: Impact of El Niño Variability on Oceanic Phytoplankton, Frontiers in Marine Science, 4, 133, https://doi.org/10.3389/fmars.2017.00133, https://www.frontiersin.org/article/10.3389/fmars.2017.00133, 2017.

Raghukumar, K., Edwards, C. A., Goebel, N. L., Broquet, G., Veneziani, M., Moore, A. M., and Zehr, J. P.: Impact of assimilating physical oceanographic data on modeled ecosystem dynamics in the California Current System, Progress in Oceanography, 138, 546 – 558, https://doi.org/https://doi.org/10.1016/j.pocean.2015.01.004, http://www.sciencedirect.com/science/article/pii/S0079661115000063, combining Modeling and Observations to Better Understand Marine Ecosystem Dynamics, 2015.

Ridley, J. K., Blockley, E. W., Keen, A. B., Rae, J. G. L., West, A. E., and Schroeder, D.: The sea ice model component of HadGEM3-GC3.1, Geoscientific Model Development, 11, 713–723, https://doi.org/10.5194/gmd-11-713-2018, https://www.geosci-model-dev.net/11/713/2018/, 2018.

Roemmich, D., Alford, M. H., Claustre, H., Johnson, K., King, B., Moum, J., Oke, P., Owens, W. B., Pouliquen, S., Purkey, S., Scanderbeg, M., Suga, T., Wijffels, S., Zilberman, N., Bakker, D., Baringer, M., Belbeoch, M., Bittig, H. C., Boss, E., Calil, P., Carse, F., Carval, T., Chai, F., Conchubhair, D. O., d'Ortenzio, F., Dall'Olmo, G., Desbruyeres, D., Fennel, K., Fer, I., Ferrari, R., Forget, G., Freeland, H., Fujiki, T., Gehlen, M., Greenan, B., Hallberg, R., Hibiya, T., Hosoda, S., Jayne, S., Jochum, M., Johnson, G. C., Kang, K., Kolodziejczyk, N., Körtzinger, A., Le Traon, P.-Y., Lenn, Y.-D., Maze, G., Mork, K. A., Morris, T., Nagai, T., Nash, J., Garabato, A. N., Olsen, A., Pattabhi, R. R., Prakash, S., Riser, S., Schmechtig, C., Schmid, C., Shroyer, E., Sterl, A., Sutton, P., Talley, L., Tanhua, T., Thierry, V., Thomalla, S., Toole, J., Troisi, A., Trull, T. W., Turton, J., Velez-Belchi, P. J., Walczowski, W., Wang, H., Wanninkhof, R., Waterhouse, A. F., Waterman, S., Watson, A., Wilson, C., Wong, A. P. S., Xu, J., and Yasuda, I.: On the Future of Argo: A Global, Full-Depth, Multi-Disciplinary Array, Frontiers in Marine Science, 6, 439, https://doi.org/10.3389/fmars.2019.00439, https://www.frontiersin.org/article/10.3389/fmars.2019.00439, 2019.

Rousseaux, C. S. and Gregg, W. W.: Climate variability and phytoplankton composition in the Pacific Ocean, Journal of Geophysical Research: Oceans, 117, https://doi.org/10.1029/2012JC008083, https://agupubs.onlinelibrary.wiley.com/doi/abs/10.1029/2012JC008083, 2012.

Rousseaux, C. S. and Gregg, W. W.: Recent decadal trends in global phytoplankton composition, Global Biogeochemical Cycles, 29, 1674–1688, https://doi.org/10.1002/2015GB005139, https://agupubs.onlinelibrary.wiley.com/doi/abs/10.1002/2015GB005139, 2015.

https://doi.org/10.5194/bg-2020-152
Preprint. Discussion started: 15 May 2020

Sathyendranath, S., Brewin, R. J., Brockmann, C., Brotas, V., Calton, B., Chuprin, A., Cipollini, P., Couto, A. B., Dingle, J., Doerffer, R., Donlon, C., Dowell, M., Farman, A., Grant, M., Groom, S., Horseman, A., Jackson, T., Krasemann, H., Lavender, S., Martinez-Vicente, V., Mazeran, C., Mélin, F., Moore, T. S., Müller, D., Regner, P., Roy, S., Steele, C. J., Steinmetz, F., Swinton, J., Taberner, M., Thompson, A., Valente, A., Zühlke, M., Brando, V. E., Feng, H., Feldman, G., Franz, B. A., Frouin, R., Gould, R. W., Hooker, S. B., Kahru, M., Kratzer, S., Mitchell, B. G., Muller-Karger, F. E., Sosik, H. M., Voss, K. J., Werdell, J., and Platt, T.: An Ocean-Colour Time Series for Use in Climate Studies: The Experience of the Ocean-Colour Climate Change Initiative (OC-CCI), Sensors, 19, https://doi.org/10.3390/s19194285, https://www.mdpi.com/1424-8220/19/19/4285, 2019.

Scaife, A. A., Arribas, A., Blockley, E., Brookshaw, A., Clark, R. T., Dunstone, N., Eade, R., Fereday, D., Folland, C. K., Gordon, M., Hermanson, L., Knight, J. R., Lea, D. J., MacLachlan, C., Maidens, A., Martin, M., Peterson, A. K., Smith, D., Vellinga, M., Wallace, E., Waters, J., and Williams, A.: Skillful long-range prediction of European and North American winters, Geophysical Research Letters, 41, 2514–2519, https://doi.org/10.1002/2014GL059637, https://agupubs.onlinelibrary.wiley.com/doi/abs/10.1002/2014GL059637, 2014.

Schartau, M., Wallhead, P., Hemmings, J., Löptien, U., Kriest, I., Krishna, S., Ward, B. A., Slawig, T., and Oschlies, A.: Reviews and syntheses: parameter identification in marine planktonic ecosystem modelling, Biogeosciences, 14, 1647–1701, https://doi.org/10.5194/bg-14-1647-2017, https://www.biogeosciences.net/14/1647/2017/, 2017.

Sellar, A. A., Jones, C. G., Mulcahy, J. P., Tang, Y., Yool, A., Wiltshire, A., O'Connor, F. M., Stringer, M., Hill, R., Palmieri, J., Woodward, S., de Mora, L., Kuhlbrodt, T., Rumbold, S. T., Kelley, D. I., Ellis, R., Johnson, C. E., Walton, J., Abraham, N. L., Andrews, M. B., Andrews, T., Archibald, A. T., Berthou, S., Burke, E., Blockley, E., Carslaw, K., Dalvi, M., Edwards, J., Folberth, G. A., Gedney, N., Griffiths, P. T., Harper, A. B., Hendry, M. A., Hewitt, A. J., Johnson, B., Jones, A., Jones, C. D., Keeble, J., Liddicoat, S., Morgenstern, O., Parker, R. J., Predoi, V., Robertson, E., Siahaan, A., Smith, R. S., Swaminathan, R., Woodhouse, M. T., Zeng, G., and Zerroukat, M.: UKESM1: Description and Evaluation of the U.K. Earth System Model, Journal of Advances in Modeling Earth Systems, 11, 4513–4558, https://doi.org/10.1029/2019MS001739, https://agupubs.onlinelibrary.wiley.com/doi/abs/10.1029/2019MS001739, 2019.

Skákala, J., Ford, D., Brewin, R. J., McEwan, R., Kay, S., Taylor, B., de Mora, L., and Ciavatta, S.: The Assimilation of Phytoplankton Functional Types for Operational Forecasting in the Northwest European Shelf, Journal of Geophysical Research: Oceans, 123, 5230–5247, https://doi.org/10.1029/2018JC014153, https://agupubs.onlinelibrary.wiley.com/doi/abs/10.1029/2018JC014153, 2018.

Storkey, D., Blockley, E. W., Furner, R., Guiavarc'h, C., Lea, D., Martin, M. J., Barciela, R. M., Hines, A., Hyder, P., and Siddorn, J. R.: Forecasting the ocean state using NEMO:The new FOAM system, Journal of Operational Oceanography, 3, 3–15, https://doi.org/10.1080/1755876X.2010.11020109, https://doi.org/10.1080/1755876X.2010.11020109, 2010.

Storkey, D., Blaker, A. T., Mathiot, P., Megann, A., Aksenov, Y., Blockley, E. W., Calvert, D., Graham, T., Hewitt, H. T., Hyder, P., Kuhlbrodt, T., Rae, J. G. L., and Sinha, B.: UK Global Ocean GO6 and GO7: a traceable hierarchy of model resolutions, Geoscientific Model Development, 11, 3187–3213, https://doi.org/10.5194/gmd-11-3187-2018, https://www.geosci-model-dev.net/11/3187/2018/, 2018.

Telszewski, M., Palacz, A., and Fischer, A.: Biogeochemical In-situ Observations - Motivation, Status and New Frontiers, in: New Frontiers in Operational Oceanography, edited by Chassignet, E. P., Pascual, A., Tintoré, J., and Verron, J., chap. 6, pp. 131–160, GODAE OceanView, 2018.

Teruzzi, A., Dobricic, S., Solidoro, C., and Cossarini, G.: A 3-D variational assimilation scheme in coupled transport-biogeochemical models: Forecast of Mediterranean biogeochemical properties, Journal of Geophysical Research: Oceans, 119, 200–217, https://doi.org/10.1002/2013JC009277, https://agupubs.onlinelibrary.wiley.com/doi/abs/10.1002/2013JC009277, 2014.

https://doi.org/10.5194/bg-2020-152
Preprint. Discussion started: 15 May 2020

Torres, R., Allen, J., and Figueiras, F.: Sequential data assimilation in an upwelling influenced estuary, Journal of Marine Systems, 60, 317 – 329, https://doi.org/https://doi.org/10.1016/j.jmarsys.2006.02.001, http://www.sciencedirect.com/science/article/pii/S0924796306000315, 2006.

Valsala, V. and Maksyutov, S.: Simulation and assimilation of global ocean pCO2 and air2̌013sea CO2 fluxes using ship observations of surface ocean pCO2 in a simplified biogeochemical offline model, Tellus B: Chemical and Physical Meteorology, 62, 821–840, https://doi.org/10.1111/j.1600-0889.2010.00495.x, https://doi.org/10.1111/j.1600-0889.2010.00495.x, 2010.

Van Leer, B.: Towards the ultimate conservative difference scheme. IV. A new approach to numerical convection, Journal of Computational Physics, 23, 276–299, 1977.

Verdy, A. and Mazloff, M. R.: A data assimilating model for estimating Southern Ocean biogeochemistry, Journal of Geophysical Research: Oceans, 122, 6968–6988, https://doi.org/10.1002/2016JC012650, https://agupubs.onlinelibrary.wiley.com/doi/abs/10.1002/2016JC012650, 2017.

Waters, J., Lea, D. J., Martin, M. J., Mirouze, I., Weaver, A., and While, J.: Implementing a variational data assimilation system in an operational 1/4 degree global ocean model, Quarterly Journal of the Royal Meteorological Society, 141, 333–349, https://doi.org/10.1002/qj.2388, https://rmets.onlinelibrary.wiley.com/doi/abs/10.1002/qj.2388, 2015.

Weaver, A. T., Vialard, J., and Anderson, D. L. T.: Three- and Four-Dimensional Variational Assimilation with a General Circulation Model of the Tropical Pacific Ocean. Part I: Formulation, Internal Diagnostics, and Consistency Checks, Monthly Weather Review, 131, 1360–1378, https://doi.org/10.1175/1520-0493(2003)131<1360:TAFVAW>2.0.CO;2, https://doi.org/10.1175/1520-0493(2003)131<1360:TAFVAW>2.0.CO;2, 2003.

Weaver, A. T., Deltel, C., Machu, E., Ricci, S., and Daget, N.: A multivariate balance operator for variational ocean data assimilation, Quarterly Journal of the Royal Meteorological Society, 131, 3605–3625, https://doi.org/10.1256/qj.05.119, https://rmets.onlinelibrary.wiley.com/doi/abs/10.1256/qj.05.119, 2005.

While, J., Totterdell, I., and Martin, M.: Assimilation of pCO_2 data into a global coupled physical-biogeochemical ocean model, Journal of Geophysical Research: Oceans, 117, https://doi.org/10.1029/2010JC006815, https://agupubs.onlinelibrary.wiley.com/doi/abs/10.1029/2010JC006815, 2012.

Wijffels, S., Roemmich, D., Monselesan, D., Church, J., and Gilson, J.: Ocean temperatures chronicle the ongoing warming of Earth, Nature Climate Change, 6, 116–118, https://doi.org/10.1038/nclimate2924, 2016.

Williams, K. D., Copsey, D., Blockley, E. W., Bodas-Salcedo, A., Calvert, D., Comer, R., Davis, P., Graham, T., Hewitt, H. T., Hill, R., Hyder, P., Ineson, S., Johns, T. C., Keen, A. B., Lee, R. W., Megann, A., Milton, S. F., Rae, J. G. L., Roberts, M. J., Scaife, A. A., Schiemann, R., Storkey, D., Thorpe, L., Watterson, I. G., Walters, D. N., West, A., Wood, R. A., Woollings, T., and Xavier, P. K.: The Met Office Global Coupled Model 3.0 and 3.1 (GC3.0 and GC3.1) Configurations, Journal of Advances in Modeling Earth Systems, 10, 357–380, https://doi.org/10.1002/2017MS001115, https://agupubs.onlinelibrary.wiley.com/doi/abs/10.1002/2017MS001115, 2017.

Yool, A., Popova, E. E., and Anderson, T. R.: MEDUSA-2.0: an intermediate complexity biogeochemical model of the marine carbon cycle for climate change and ocean acidification studies, Geoscientific Model Development, 6, 1767–1811, https://doi.org/10.5194/gmd-6-1767-2013, https://www.geosci-model-dev.net/6/1767/2013/, 2013.

Yool, A., Palmiéri, J., Jones, C. G., Sellar, A. A., de Mora, L., Kuhlbrodt, T., Popova, E. E., Mulcahy, J. P., Wiltshire, A., Rumbold, S. T., Stringer, M., Hill, R. S. R., Tang, Y., Walton, J., Blaker, A., Nurser, A. J. G., Coward, A. C., Hirschi, J., Woodward, S., Kelley, D. I., Ellis, R., and Rumbold-Jones, S.: Spin-up of UK Earth System Model 1 (UKESM1) for CMIP6, Journal of Advances in Modeling

Earth Systems, n/a, e2019MS001 933, https://doi.org/10.1029/2019MS001933, https://agupubs.onlinelibrary.wiley.com/doi/abs/10.1029/2019MS001933, e2019MS001933 2019MS001933, 2020.

Yu, L., Fennel, K., Bertino, L., Gharamti, M. E., and Thompson, K. R.: Insights on multivariate updates of physical and biogeochemical ocean variables using an Ensemble Kalman Filter and an idealized model of upwelling, Ocean Modelling, 126, 13 – 28, https://doi.org/https://doi.org/10.1016/j.ocemod.2018.04.005, http://www.sciencedirect.com/science/article/pii/S1463500318301318, 2018.

Yu, L., Fennel, K., Wang, B., Laurent, A., Thompson, K. R., and Shay, L. K.: Evaluation of nonidentical versus identical twin approaches for observation impact assessments: an ensemble-Kalman-filter-based ocean assimilation application for the Gulf of Mexico, Ocean Science, 15, 1801–1814, https://doi.org/10.5194/os-15-1801-2019, https://www.ocean-sci.net/15/1801/2019/, 2019.

Zalesak, S. T.: Fully multidimensional flux-corrected transport algorithms for fluids, Journal of Computational Physics, 31, 335–362, 1979.